Performance Evaluation of The VSC-Interfaced Distributed Resource Models

by

Gorken Gumustekin

A thesis submitted in conformity with the requirements
for the degree of Master of Applied Science
Graduate Department of Electrical and Computer Engineering
University of Toronto

Abstract

Performance Evaluation of The VSC-Interfaced Distributed Resource Models

Gorken Gumustekin
Master of Applied Science
Graduate Department of Electrical and Computer Engineering
University of Toronto
2016

The voltage-sourced converter (VSC) is the mostly used converter configuration for grid integration of distributed resources, i.e., generation and storage units. For such applications, the VSC is conventionally controlled by means of an inner-current controller that operates the VSC based on the desired VSC current to meet the system operational requirements. In compliance with the principles of the inner-current controller, the current-injection model has been widely used to represent the VSC impact studied of the grid-integrated DG.

This thesis investigates the validity of the VSC current-injection model under the unbalanced conditions of feeder and low short-circuit ratios. The objective is establish the degree of accuracy of impact studies based on the current-injection model.

A test system has been selected and the steady-state and transient-response of a 1.5 MW VSC based detailed switched-model and the current-injection model under various unbalanced and the system short-circuit capacity have been investigated and compared.

Acknowledgements

First and foremost, I would like to give sincere thanks to my supervisor Prof. Reza Iravani for his valuable time, continuous support and guidance throughout my masters degree education. I cannot thank him fairly enough for his encouragement and kindly assistance.

I would also like to thank Dr. Milan Graovac and Mr. Xiaolin Wang for their many hours of weekly discussion which has helped my understanding of the concepts in this thesis. Their endless help is a critical factor for this thesis.

Moreover, I am thankful to my country for supporting me during Master.

I would like to extend my deepest wholehearted thanks to my parents for their faithful devotions for me.

Contents

List of Tables

List of Figures

List of Abbreviations

VSC	Voltage Source Converter
SCR	Short-Circuit Ratio
PLL	Phase Locked Loop
DG	Distributed Generation
VSC	Voltage Source Converter
DN	Distribution Network
AMI	Advanced Metering/Monitoring Infrastructure
VAR	Volt-Ampere Reactive
DC	Direct Current
AC	Alternating Current
HVDC	High-Voltage Direct Current
SC_{MVA}	Short Circuit MVA
POI	Point of Interconnection
SPWM	Sinusoidal Pulse Width Modulation
IEEE	Institute of Electrical and Electronics Engineers
LV	Low Voltage
NEMA	National Equipment Manufacturer's Association
LVUR	Line Voltage Unbalance Rate
PVUR	Phase Voltage Unbalance Rate

Chapter 1

Introduction

1.1 Problem Statement

Recent and ongoing developments in power electronics economical viability of alternative energy resources, e.g., wind and solar power [1, 2], and energy storage media, e.g., battery and flywheel storage systems, all indicate significant proliferation of voltage-sourced converter (VSC) units in the electric power grid [3]-[6]. In this context, the VSC serves as the electrical interface medium between a source/storage system and it host utility grid. Depending on the rated power and functions of the source/storage system, the corresponding VSC unit can be either a single-phase or three-phase unit. This documents is concerned with three-phase VSC units. The three-phase VSC unit has been widely used to interface a source/storage system of few tens of kW up to multi-MW at voltage levels of a few hundred volts to tens of kV. Except for HVDC system applications, a VSC is cascaded with a three-phase transformer which can have a variety of winding configurations.

The inherent operational characteristic of the VSC enables it to provide fast control over multiple parameters, e.g., instantaneous real/reactive power (PQ mode), DC side voltage, AC side voltage phasor, and frequency [7, 8]. This document is concerned with the scenarios that a VSC operates in the PQ-mode and can inject/absorb real- and reactive-power in four quadrants. This mode is the most widely adopted mode of operation at the distribution-class voltage levels, e.g., 480-V to 69-kV, and includes VSCs from a few tens of kW up to 2.5 MW.

For the utility grid applications, a VSC can be operated either as a voltage-controlled unit or a current-controlled unit with respect to the AC side. The latter is the preferred mode since it provides current-limit capability and provides embedded over-current protection for the electronic switches during the utility grid abnormal scenarios, e.g., faults and switching events. In this document we adopt the VSC under the current-controlled mode of operation in which the inner current control-loop controls the injected current by the VSC into the grid and the outer control loop provides the required current reference values to meet PQ exchange of the overall unit, i.e., the source/storage and the VSC interface.

The underlying assumption in the VSC modeling, control, and performance evaluation by the vendors and power utilities is that the host grid is a three-phase balanced system. This is a fairly valid assumption for three-phase transmission-level system but not for the distribution level systems. The distribution-level system is subject to a significant degree of asymmetry under steady-state conditions due to (i) untransposed lines, single-phase laterals,and single-phase load and/or generation. This asymmetry is even more pronounced under transient scenarios, e.g., a single-phase to ground fault and its subsequent single-pole breaker operation and re-closure actions.

Prior to installation, commisioning, and operation of a VSC-interfaced generation/storage unit, the power utility performs multiple impact studies to guarantee sound operation of the unit its host grid under a wide range of system scenarios. These studies conventionally utilize the positive-sequence based vendor model of the VSC and its control which is designed under the assumption of balanced grid. Therefore, the main concern that has been raised by the utility industry includes:

- Do positive-sequence based generic models of the VSC [9] (and its control) provide adequately accurate response under (realistic) unbalanced conditions of the distribution grid ?
- Is there a specific unbalanced threshold limit beyond which the positive-sequence based VSC models are not adequately accurate ?
- Can the VSC be equipped with additional controller to (i) mitigate the impact of system unbalance on the VSC operation, and/or (ii) even counteract the system unbalanced behavior?

The above issues have neither been fully answered in a systematic way nor been comprehensively understood, particularly where multiple VSC units operate in close electrical proximity of each other. The focus of this work to address the first two concerns. Providing meaningful response to the latter question requires establishment of ”performance criteria” which is beyond the scope of this work.

1.2 Thesis Objectives

The objectives of this work include:

(a) Identification of a realistic distribution system (feeder) down stream to the distribution transformer station for the studies.

(b) Developing the steady-state power flow model and transient model of the system of item (a) (in the PSCAD platform) for the required studies.

(c) Selection of a VSC-interfaced distributed generation system and development of its positive-sequence model to be incorporated in the system models of item (b) above.

(d) Comprehensive case studies, under steady-state and transient scenarios, to establish the VSC response under balanced and unbalanced conditions.

1.3 Thesis Layout

The structure of this thesis is as follows:

Chapter 2 introduce a distribution feeder which is used in the rest of the thesis for the case studies. Chapter 2 also presents a generic structure for a three-phase VSC unit and its control to integrate distributed generation/storage in the test feeder. Finally chapter 2 introduces widely used models of the VSCs for the case studies.

Chapter 3 adopts the VSC models of chapter 2 and evaluates performance of models under steady conditions and provides a comparison of performances.

Chapter 4 is primarily concerned with the performances of the VSC models of chapter 2 under transient scenarios. Both balanced and unbalanced faults and the subsequent switching events are considered.

Chapter 5 provides the conclusions of the studied cases and the future work in the area.

Chapter 2

Study System

2.1 Introduction

This chapter introduces distribution power system, i.e., a feeder down stream of a transformer station, as the system that incorporates a VSC-interfaced generation unit [10, 11] for the study cases. This chapter also introduces the details of the VSC-interfaced unit and its control system. The introduced study system is used in the subsequent chapters to investigate the behavior of the VSC unit under the distribution system balanced/unbalanced conditions [12, 13].

2.2 Distribution Feeder

Figure 2.1 shows a schematic diagram of the distribution feeder for the investigations [14, 15]. The main trunk of the feeder is a 27.6 kV overhead line which is supplied by the main grid. The main grid is represented in Figure 2.1 by an equivalent 27.6 kV voltage source with the short circuit capacity (SC_{MVA}) of 885.33 MVA. The feeder supplies multiple loads by lateral overhead lines either directly or through transformers. Figure 2.1 also shows that the laterals can be three-phase, two-phase, and single-phase [16, 17]. Therefore, the feeder is an unbalanced system. The main overhead line of the feeder is not transposed and thus is not symmetrical. The feeder also includes a voltage regulating transformer, i.e., transformer T2. The parameters of the feeder are given in Appendix A . The feeder is also equipped with a three-phase 1.5 MW, 370 V distributed generation unit, e.g., a solar-PV unit, which is interfaced to the feeder at the point of interconnection (POI) through a three-phase transformer and a three-phase two-level VSC unit as will be described in the following sections.

For some study cases where the feeder characteristics at POI need to be re-adjusted to highlight the impact of the specific scenarios, instead of the configuration of Figure 2.1, it equivalents with respect to POI, as shown in Figure 2.2, are used. In the system of Figure 2.2, (i) the main system of Figure 2.1 and the feeder section between the main feeder and POI is replaced by its thevenin equivalent with respect to POI, and (ii) the feeder downstream from POI is replaced by a passive impedance (assuming there is no generation beyond POI in the feeder).

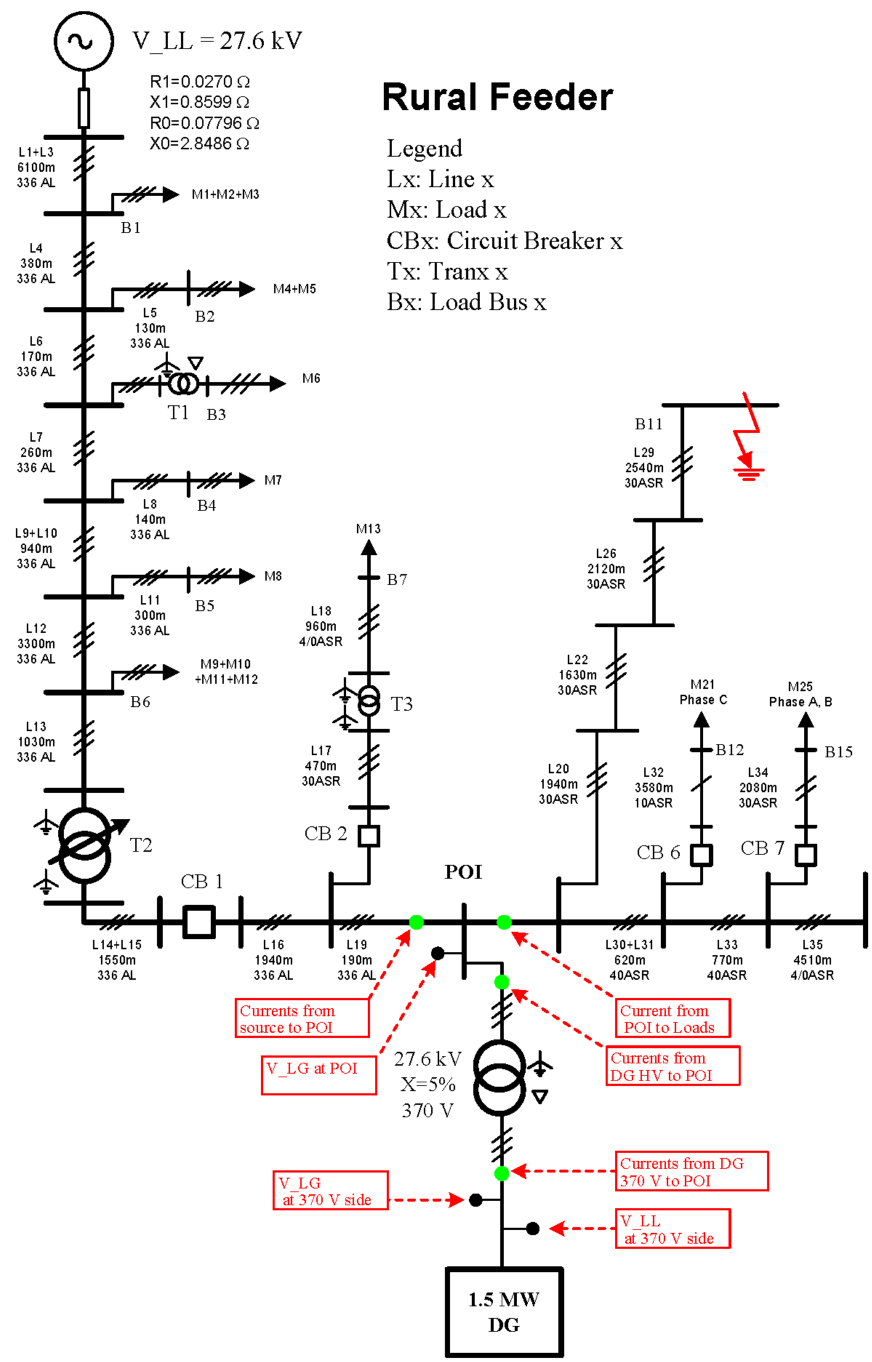

Figure 2.1: One-line Diagram of the Study System

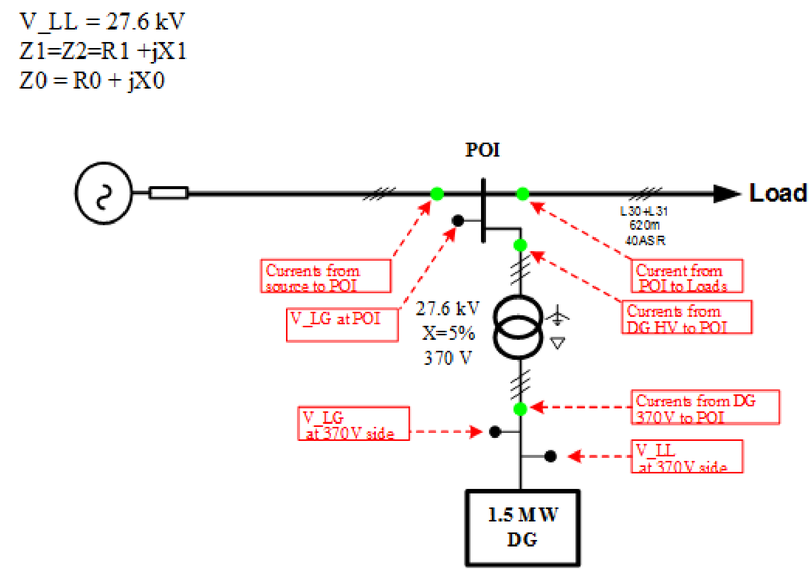

Figure 2.2: One-line Diagram of the Study System represented by two equivalents with respect to right- and left-side of POI

2.3 Distributed Generation Unit

Figure 2.3 shows a schematic diagram of the distributed generation system [18], e.g., a solar-PV unit, including its VSC-interface.

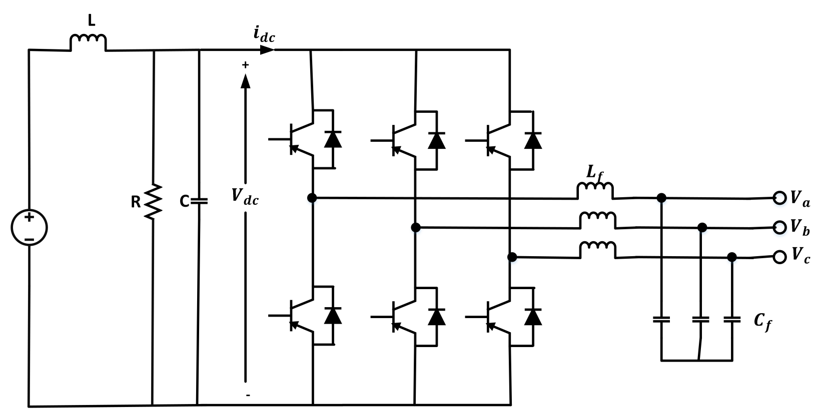

Figure 2.3: Schematic Diagram of the VSC

The DC-side is represented by (i) a DC voltage source, (ii) L and R, respectively, represent the inductance and the equivalent internal resistance of the DC-side interface reactor, and (iii) DC-capacitor C. The VSC is a conventional IGBT-based two-level configuration. The VSC operates based on a sinusoidal pulse width modulation (SPWM) switching strategy at the switching frequency of 3.06 kHz. The AC side filter is an LC filter in each phase to meet the IEEE harmonic content requirements [19]. It should be noted that converter transformer also participates in the filter action and practically the filter in each phase is an asymmetrical "T" type filter [20]. The parameters of the configuration of Figure 2.3 are given Table 2.1.

Table 2.1: VSC parameters

DC-side	
Parameters	Values
L	1 uH
R	20000 ohm
C	12000 uF
AC-side	
Parameters	Values
Lf	27 uH
Cf	2900 uF

Figure 2.4 shows a block diagram of the inner-loop current-controller of the VSC [12], and the outer-loop control system determines the reference currents for the inner-loop, i.e., I_{dref} and I_{qref}, based on the desired control objective [8]. Presently, most electronically-coupled DG units operate based on real- and reactive-power injection and this strategy is adopted in this work for the outer-controller. The VSC unit is synchronized to the transformer low-voltage (LV) side by a phase-locked loop (PLL) system [13, 21]. The PLL provides the synchronization to the positive-sequence voltage of the transformer low voltage (LV) side.

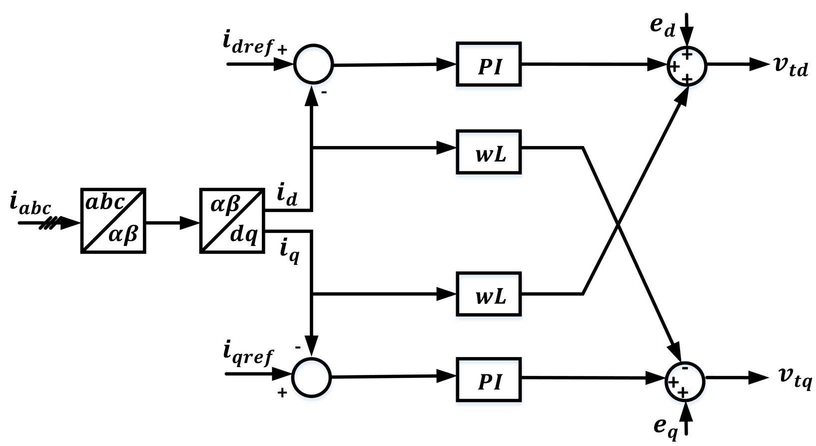

Figure 2.4: Inner-loop Current Controller

Table 2.2: PI Controller Datas

Parameters	**Values**
Proportional Gain	0.022
Integral Time Constant	0.5 s

2.4 System Model

For the purpose of the studies reported in the following chapters, the overall system is modeled in the EMTDC/PSCAD platform as follows.

2.4.1 Feeder Model

The feeder is represented as a three-phase system (and two-phase and single-phase where applicable). Each line section is represented by lumped RL elements including sequence parameters. Each transformer is represented as a linear three-phase transformer according to the corresponding winding structure of Figure 2.1. The network equivalent in Figure 2.1 is represented by a three-phase voltage source including sequence impedances. This modeling process also used when the feeder system of Figure 2.2 was used.

2.4.2 VSC System Switch-Model

The detailed converter system includes sections described in section 2.3. The power circuity of the converter system, i.e., that of Figure 2.3, is modeled in the EMTDC/PSCAD platform, in which the VSC electronic switches are represented as ideal on-off switches.The control system of the VSC converter, i.e., those of Figures 2.4 and the outer-loop controller, including the synchronization PLL are modeled in the EMTDC/PSCAD software tool. This model represents the dynamics of the converter system and in steady-state conditions it provides both the fundamental-frequency response of the converter system and the switching harmonics. Hereafter we refer to this model of the VSC system as the "switched-model" and it provides a benchmark for evaluation of the accuracy of the other VSC system models as described in the following sections.

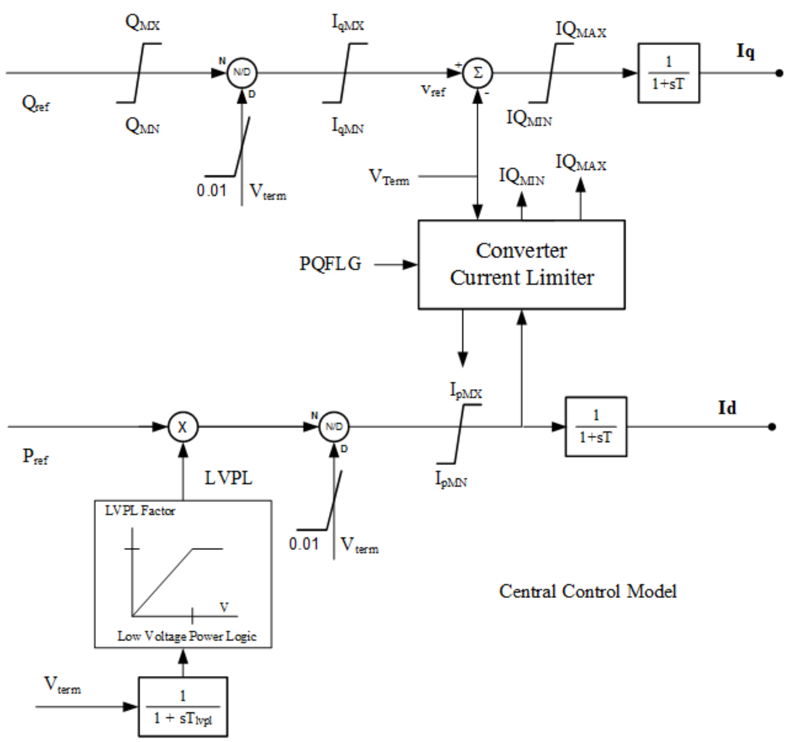

Figure 2.5: VSC current-sourced model

2.4.3 VSC Current-Sourced (Current-Injection) Model

In this modeling approach the VSC of Figure 2.3, excluding the AC-side filter, the inner-loop current controller of Figure 2.4 and the outer real-/reactive-power controllers are combined and represented as a current-controlled current-source as shown in Figure 2.5 which produce I_d and I_q. This source injects into the system, Figure 2.6, the three-phase current I_a, I_b, and I_c associated with the reference I_d and I_q current components that are generated by the model of Figure 2.5. Thus it injects currents into the system associated with the desired real- and reactive-power components. Hereafter, this model is referred to "current-sourced model" or "current-injection model".

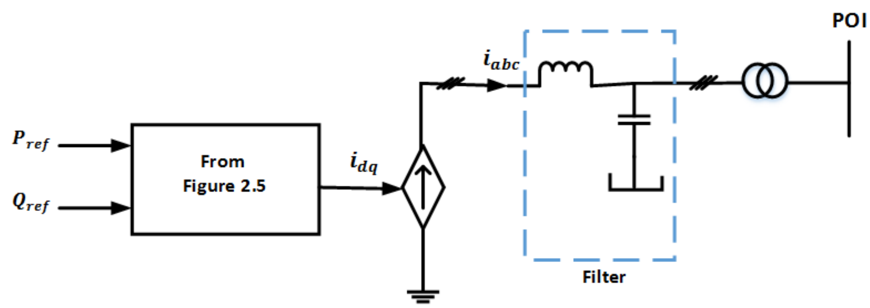

Figure 2.6: Integration of Current-Sourced Model of VSC with the host AC system

It should be noted that the current-sourced model represents the steady-state and dynamics of the VSC system only at the fundamental frequency component of its AC side. The current-sourced model of Figure 2.6 is widely adopted by the stakeholders to perform system impact studies. The objective of this work is to establish if the response of this model accurately agrees with that of the switched-model of section 2.4.2, particularly under unbalanced and/or low short-circuit ratio (SCR) conditions.

2.4.4 VSC Voltage-Sourced Model

Another option for an equivalent model of the VSC system is to represent it as a current-controlled voltage source, as shown in Figure 2.7.

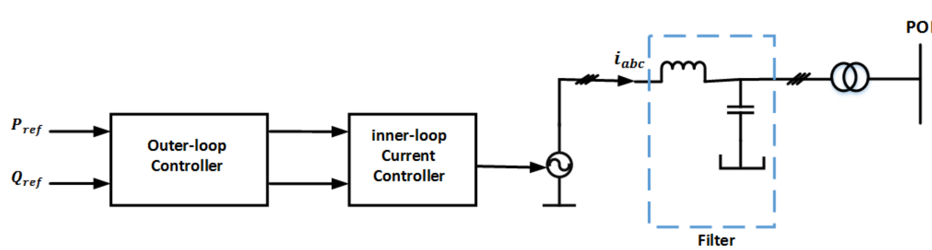

Figure 2.7: Current-Controlled Voltage-Source Model

The voltage source of Figure 2.7 is current-controlled such that it meets the requirements of active- and reactive-power reference values and the inner-loop current controller. The main drawback of this model as compared with that of Figure 2.6 is that it requires details of the inner-loop current controller which often is not provided by the VSC vendor and thus is not used in this work any further.

2.5 Definition of System Unbalanced

The three widely used and common definitions of voltage unbalance are as follows.

NEMA (National Equipment Manufacturer's Association) Definition : The NEMA definition of voltage imbalance also known as the line voltage unbalance rate (LVUR) [22] is given by

$$LVUR(\%) = \frac{max\ voltage\ deviation\ from\ the\ average\ line\ voltage}{average\ line\ voltage} 100. \tag{2.1}$$

IEEE Definition: The IEEE definition [23] of voltage unbalance, also known as phase voltage unbalance rate (PVUR) is given by

$$PVUR(\%) = \frac{max\ voltage\ deviation\ from\ the\ average\ phase\ voltage}{average\ phase\ voltage} 100. \tag{2.2}$$

The IEEE definition of voltage unbalance is similar to that of NEMA, and the only difference is that the IEEE uses phase voltage rather than the line-to-line voltage.

True Definition : This definition is expressed as the ratio of the negative-sequence voltage component, to the positive-sequence voltage component, [19],[23]-[25],

$$unbalance(\%) = \frac{V_{negative-sequence}}{V_{positive-sequence}} 100. \tag{2.3}$$

The true definition is used in this thesis because it is more widely used in the literature as compared with the other two definitions. The typical characteristic of imbalance, based the true definition, are given in Table 2.3.

Table 2.3: Typical Characteristic of Voltage and Current Imbalance

	System Condition	Voltage and current Magnitude
Voltage imbalance	steady-state	2%
Current imbalance	steady-state	30%

2.6 Summary

This chapter introduces the test system and the corresponding component model for case studies in the PSCAD/EMTDC platform. The test system is a 27-kV rural distribution feeder which includes multiple three-, two- and single-phase loads and hosts a 1.5 MW VSC-interfaced distributed generation unit. The unit is represented based on two models, i.e., the switched-model and the current-sourced model. The switched-model is the most accurate representation for system studies within the frequency range of about 0-50 khz while the current-sourced model only represents the fundamental-frequency behaviour of the unit.

Chapter 3

Steady-State Responses of VSC Models

3.1 Introduction

The objectives of this chapter is to investigate the behavior of a three-phase, three wires, inverter-interfaced unit under unbalanced, steady-state system conditions. The study system is the rural distribution feeder introduced in the Chapter 2 and its single-line diagram is repeated in Fig. 3.1 for the ease of reference. The VSC-integrated system is the 1.5 MW, 370 V system that was also introduced in Chapter 2. The inverter-based system is represented by two modals, i.e., the switched-model and the current-injection modal in the PSCAD/EMTDC software platform. The corresponding results are compared to establish the degree of accuracy of the current-injection model as compared with detailed switched-model, with report to the fundamental frequency component

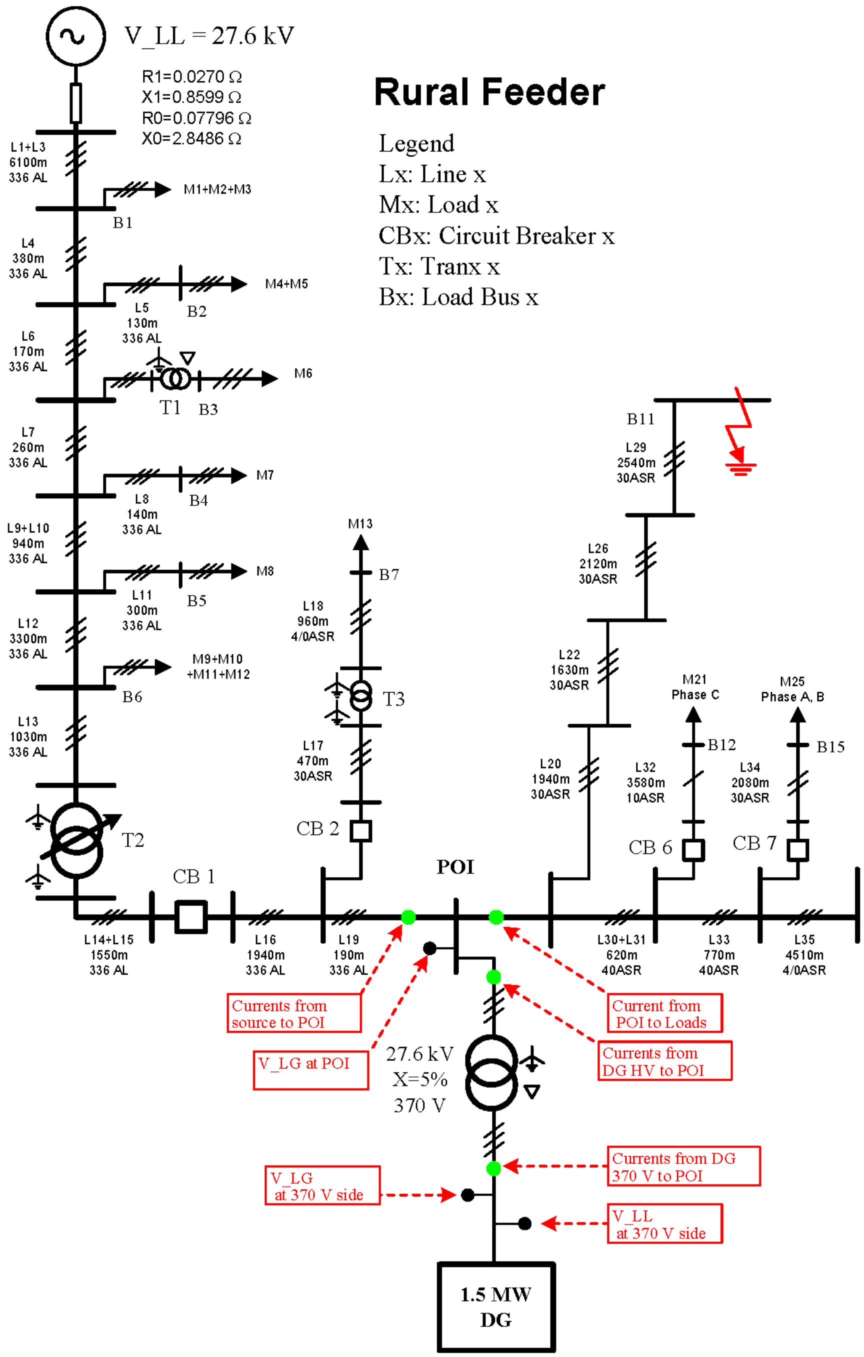

Figure 3.1: One-Line Diagram of the Study System

3.2 Component Models

The reported studies in this chapter are based on time-domain simulation of the study system of Figure 3.1 in the PSCAD/EMTDC platform. The components of the study system of Figure 3.1 are developed in the PSCAD/EMTDC as described in Chapter 2. For each case study, the VSC of unit is represented once by the switched-model and once by the current-injection model. Since the switched-model captures the details of the VSC behaviour, its response is used as the reference. Comparison of the results from the VSC current-injection model with those of the switched-model are used to evaluate the accuracy of the current-injection model.

3.3 Study Results

For each of the two models of the VSC unit, the studies are conducted for various scenerios that pratically can be experienced, i.e.,

- balanced or unbalanced load conditions,
- (almost) resistive or RL loads,
- different values of short-circuit capacity at POI of Figure 3.1

The results are tabulated and compared in the following sections. In the reported studies, the degree of the system imbalance of the voltage (current) is specified by the ratio of the negative-sequence voltage (current) amplitude to the positive-sequence voltage (current) amplitude [19], [23]-[25] and the acceptable limits are provided in Table 2.2 of Chapter 2. To create a specific level of "unbalanced" at POI, the down-stream load with respect to POI is made unbalanced, e.g., corresponding to 2% unbalanced voltage at POI.

3.3.1 Case-1 : Short-Circuit Capacity of 85 MVA at POI

The main grid short-circuit MVA (SC_{MVA}) at the distribution substation is about 885 MVA. Due to the feeder impedance between the substation and POI of Fig. 3.1, the SC_{MVA} at POI is 85 MVA.

Case-1.1 : Balanced Resistive Load (3 MW)

Table 3.1 shows the study results under the balanced resistive loads of 3 MW (downstream to POI) when the VSC unit is not in service. Table 3.1 indicates, as expected, the three phase POI voltages are balanced. Table 3.1 also shows various measured currents/voltages of the study system which are used as the base cases to evaluate the impact of system unbalanced operation.

Table 3.2 shows the study results when the same resistive balanced load of 3 MW is in service, and current-injection model (without LC filter) of VSC unit is connected at POI, as shown in Figure 3.1. Table 3.2 indicates that, as expected, the three-phase POI voltages remain balanced.

Table 3.3 illustrates the study results under the same resistive balanced load of 3 MW when the switched-model of VSC unit is connected to the main feeder at POI. Similar to the two previous cases of Table 3.1 and Table 3.2, the results of Table 3.3 also indicate that voltages of the three-phase at POI are balanced.

Table 3.1 to 3.3 conclude that for the given system $SC_{MVA} = 85$ both models provide practically identical results and thus the current-injection model accurately represents the VSC.

Table 3.1: Balanced resistive load of 3 MW, VSC unit not in service

Monitored Variable	RMS Phase Magnitude			RMS Sequence Magnitude			Sequence Angle		
	A	B	C	Positive	Negative	Zero	Positive	Negative	Zero
	(kV)	(kV)	(kV)	(kV)	(kV)	(kV)	(Degree)	(Degree)	(Degree)
L-G POI Voltage (27.6-kV Side)	15.46	15.46	15.46	15.46	0	0	-5.56	0	0
L-L Voltage (370-V Side)	0.359	0.359	0.359	0.359	0	0	-5.67	0	0
	RMS Phase Magnitude			RMS Sequence Magnitude			Sequence Angle		
	(kA)	(kA)	(kA)	(kA)	(kA)	(kA)	(Degree)	(Degree)	(Degree)
Source to POI Current (27.6 kV Side)	0.0608	0.0608	0.0608	0.0608	0	0	-4.82	0	0
POI to Loads Current (27.6 kV Side)	0.0608	0.0608	0.0608	0.0608	0	0	-4.65	0	0
VSC to POI Current (27.6 kV Side)	0	0	0	0	0	0	0	0	0
VSC to POI Current (370 V Side)	0	0	0	0	0	0	0	0	0
VSC Power Output	Source to POI			POI to Loads			VSC to POI (27.6-kV side)		
	P	Q		P	Q		P	Q	
	(kW)	(kVar)		(kW)	(kVar)		(kW)	(kVar)	
	2820	9		2820	0		0	-9	

Table 3.2: Balanced resistive load of 3 MW, Current-injection model (without LC filter) of VSC unit in service

Monitored Variable	RMS Phase Magnitude			RMS Sequence Magnitude			Sequence Angle		
	A	B	C	Positive	Negative	Zero	Positive	Negative	Zero
	(kV)	(kV)	(kV)	(kV)	(kV)	(kV)	(Degree)	(Degree)	(Degree)
L-G POI Voltage (27.6-kV Side)	15.55	15.55	15.55	15.55	0	0	-4.29	0	0
L-L Voltage (370-V Side)	0.361	0.361	0.361	0.361	0	0	-1.78	0	0
	RMS Phase Magnitude			RMS Sequence Magnitude			Sequence Angle		
	(kA)	(kA)	(kA)	(kA)	(kA)	(kA)	(Degree)	(Degree)	(Degree)
Source to POI Current (27.6 kV Side)	0.029	0.029	0.029	0.029	0	0	-5.45	0	0
POI to Loads Current (27.6 kV Side)	0.061	0.061	0.061	0.061	0	0	-3.37	0	0
VSC to POI Current (27.6 kV Side)	0.032	0.032	0.032	0.032	0	0	-1.5	0	0
VSC to POI Current (370 V Side)	2.4	2.4	2.4	2.4	0	0	-31.82	0	0
VSC Power Output	Source to POI			POI to Loads			VSC to POI (27.6-kV side)		
	P	Q		P	Q		P	Q	
	(kW)	(kVar)		(kW)	(kVar)		(kW)	(kVar)	
	1353	28		2853	-45		1500	-73	

Table 3.3: Balanced resistive load of 3 MW, Switched-model of VSC unit in service

Monitored Variable	RMS Phase Magnitude			RMS Sequence Magnitude			Sequence Angle		
	A	B	C	Positive	Negative	Zero	Positive	Negative	Zero
	(kV)	(kV)	(kV)	(kV)	(kV)	(kV)	(Degree)	(Degree)	(Degree)
L-G POI Voltage (27.6-kV Side)	15.56	15.56	15.56	15.56	0	0	-4.29	0	0
L-L Voltage (370-V Side)	0.361	0.361	0.361	0.361	0	0	-1.75	0	0
	RMS Phase Magnitude			RMS Sequence Magnitude			Sequence Angle		
	(kA)	(kA)	(kA)	(kA)	(kA)	(kA)	(Degree)	(Degree)	(Degree)
Source to POI Current (27.6 kV Side)	0.0288	0.0288	0.0288	0.0288	0	0	-6.9	0	0
POI to Loads Current (27.6 kV Side)	0.0611	0.0612	0.0612	0.0612	0	0	-3.68	0	0
VSC to POI Current (27.6 kV Side)	0.0324	0.0324	0.0324	0.0324	0	0	-0.01	0	0
VSC to POI Current (370 V Side)	2.417	2.423	2.415	2.417	0	0	-30.4	0	0
VSC Power Output	Source to POI			POI to Loads			VSC to POI (27.6 kV side)		
	P	Q		P	Q		P	Q	
	(kW)	(kVar)		(kW)	(kVar)		(kW)	(kVar)	
	1345	-3		2856	-46		1512	-43	

Case-1.2 : Unbalanced Resistive Load (3.5 MW)

In this case study, the overall load of the feeder is adjusted to 3.5 MW which correspond to 1 MW single-phase load (phase A) and 2.5 MW two-phase load connected to phases B and C to make system unbalance. Table 3.4 shows the study results under the unbalanced resistive load of 3.5 MW when the VSC unit is not in service. Due to the unbalanced loads, the degree of POI voltage imbalance is 1.91%, and the degree of current imbalance is 37.06%.

Table 3.5 shows the study results for the same unbalanced resistive load when the VSC unit is in service and represented by the current-injection model (without LC filter), and injects 1.5 MW power in the system at POI. Table 3.5 shows that in spite of the presence of the VSC unit in the system, the voltage imbalance at POI remains identical to that of the previous case, as shown in Table 3.4. However, the degree of current imbalance (current from source to POI) increased from 37.06% (Table 3.4) to 67.52% (Table 3.5). The reason is that part of the balanced-current of the load is supplied by the VSC unit, and thus the balanced-current drawn by the load from the grid, through positive-sequence current at branch form source to POI is reduced, and thus the degree of imbalance is increased.

Table 3.6 presents the study results corresponding to the previous scenerio when the VSC unit is represented by the switching-model for the studies. Comparison of the results of Table 3.5 and 3.6 indicates that:

- the degrees of voltage imbalance at POI for both cases are practically the same, i.e. 1.91%.
- the degrees of current imbalance (from source to POI) for both cases are the same, i.e. 67.8%.

Table 3.4 and 3.6 conclude that both models of the VSC unit, subject to resistive unbalanced load scenarios, under steady-state conditions, behave the same and can be used interchangebly.

Table 3.4: Unbalanced resistive load of 3.5 MW, VSC unit not in service

Monitored Variable	RMS Phase Magnitude			RMS Sequence Magnitude			Sequence Angle		
	A	B	C	Positive	Negative	Zero	Positive	Negative	Zero
	(kV)	(kV)	(kV)	(kV)	(kV)	(kV)	(Degree)	(Degree)	(Degree)
L-G POI Voltage (27.6-kV Side)	15.49	15.75	15	15.41	0.295	0.249	-5.55	106.26	-46.51
	Voltage unbalanced (%) = 1.91								
L-L Voltage (370-V Side)	0.355	0.365	0.354	0.358	0.0068	0	-6.06	106.14	0
	Voltage unbalanced (%) = 1.90								
	RMS Phase Magnitude			RMS Sequence Magnitude			Sequence Angle		
	(kA)	(kA)	(kA)	(kA)	(kA)	(kA)	(Degree)	(Degree)	(Degree)
Source to POI Current (27.6 kV Side)	0.054	0.063	0.102	0.0707	0.0262	0.009	-6.02	-148.1	43.51
	Current unbalanced (%) = 37.06								
POI to Loads Current (27.6 kV Side)	0.0608	0.054	0.108	0.0707	0.0262	0.0204	-5.87	-148.1	51.87
	Current unbalanced (%) = 37.06								
VSC to POI Current (27.6 kV Side)	0.0118	0.0118	0.0116	0	0	0.0118	0	0	43.52
VSC to POI Current (370 V Side)	0	0	0	0	0	0	0	0	0
VSC Power Output	Source to POI			POI to Loads			VSC to POI (27.6 kV side)		
	P	Q		P	Q		P	Q	
	(kW)	(kVar)		(kW)	(kVar)		(kW)	(kVar)	
	3260	27		3260	20		0	-7	

Table 3.5: Unbalanced resistive load of 3.5 MW, Current-injection model (without LC filter) of VSC unit in service

Monitored Variable	RMS Phase Magnitude			RMS Sequence Magnitude			Sequence Angle		
	A	B	C	Positive	Negative	Zero	Positive	Negative	Zero
	(kV)	(kV)	(kV)	(kV)	(kV)	(kV)	(Degree)	(Degree)	(Degree)
L-G POI Voltage (27.6-kV Side)	15.58	15.85	15.1	15.52	0.297	0.25	-4.69	107.5	-45.26
	Voltage unbalanced (%) = 1.91								
L-L Voltage (370-V Side)	0.358	0.368	0.355	0.361	0.007	0	-2.15	107.5	0
	Voltage unbalanced (%) = 1.94								
	RMS Phase Magnitude			RMS Sequence Magnitude			Sequence Angle		
	(kA)	(kA)	(kA)	(kA)	(kA)	(kA)	(Degree)	(Degree)	(Degree)
Source to POI Current (27.6 kV Side)	0.023	0.036	0.071	0.0391	0.0264	0.009	-6.9	-146.8	64.11
	Current unbalanced (%) = 67.52								
POI to Loads Current (27.6 kV Side)	0.061	0.054	0.109	0.0712	0.0264	0.0206	-4.62	-146.8	53.13
	Current unbalanced (%) = 37.08								
VSC to POI Current (27.6 kV Side)	0.041	0.021	0.037	0.0322	0	0.012	-1.8	0	44.77
	Current unbalanced (%) = 0								
VSC to POI Current (370 V Side)	2.4	2.4	2.4	2.4	0	0	-32.01	0	0
	Current unbalanced (%) = 0								
VSC Power Output	Source to POI			POI to Loads			VSC to POI (27.6 kV side)		
	P	Q		P	Q		P	Q	
	(kW)	(kVar)		(kW)	(kVar)		(kW)	(kVar)	
	1810	20		3310	20		1496	0	

Table 3.6: Unbalanced resistive load of 3.5 MW, Switched-model of VSC unit in service

Monitored Variable	RMS Phase Magnitude			RMS Sequence Magnitude			Sequence Angle		
	A	B	C	Positive	Negative	Zero	Positive	Negative	Zero
	(kV)	(kV)	(kV)	(kV)	(kV)	(kV)	(Degree)	(Degree)	(Degree)
L-G POI Voltage (27.6-kV Side)	15.6	15.85	15.09	15.51	0.299	0.25	-4.67	107.49	-45.25
	Voltage unbalanced (%) = 1.93								
L-L Voltage (370-V Side)	0.357	0.366	0.355	0.359	0.007	0	-2.12	107.51	0
	Voltage unbalanced (%) = 1.95								
	RMS Phase Magnitude			RMS Sequence Magnitude			Sequence Angle		
	(kA)	(kA)	(kA)	(kA)	(kA)	(kA)	(Degree)	(Degree)	(Degree)
Source to POI Current (27.6 kV Side)	0.023	0.036	0.071	0.0387	0.0265	0.009	-8.09	-146.8	64.14
	Current unbalanced (%) = 68.48								
POI to Loads Current (27.6 kV Side)	0.0613	0.0542	0.1089	0.0711	0.0263	0.0206	-4.59	-146.8	53.1
	Current unbalanced (%) = 36.99								
VSC to POI Current (27.6 kV Side)	0.0416	0.0212	0.0377	0.0325	0	0.0118	-0.41	0	44.8
	Current unbalanced (%) = 0								
VSC to POI Current (370 V Side)	2.423	2.433	2.412	2.42	0.0098	0	-30.8	20	0
	Current unbalanced (%) = 0.40								
VSC Power Output	Source to POI			POI to Loads			VSC to POI (27.6 kV side)		
	P	Q		P	Q		P	Q	
	(kW)	(kVar)		(kW)	(kVar)		(kW)	(kVar)	
	1815	60		3300	-20		1507	-40	

Case-1.3 : Balanced RL Load (3 MVA, 0.9 lagging power factor)

The study results presented in Table 3.7 correspond to balanced RL (resistance-inductance) load of 3 MVA at lagging power factor of 0.9 when the VSC unit is not in service. Table 3.7 shows, as expected, the three-phase voltage at POI is balanced.

Table 3.8 and Table 3.9 show the study results under the same grid condition and the same load connection of Table 3.7 when the VSC unit is in service and represented by the current-injection model (without LC filter) and switched-model with 1.5 MW power injection at POI. Table 3.8 and Table 3.9 indicate, as expected, the three-phase POI voltages remain balanced. Close agreement between the corresponding results of Table 3.8 and Table 3.9 indicates that current-injection model is an accurate representation of the VSC for the given scenario.

Table 3.7: Balanced RL load of 3 MVA (pf:0.9), VSC unit not in service

Monitored Variable	RMS Phase Magnitude			RMS Sequence Magnitude			Sequence Angle		
	A	B	C	Positive	Negative	Zero	Positive	Negative	Zero
	(kV)	(kV)	(kV)	(kV)	(kV)	(kV)	(Degree)	(Degree)	(Degree)
L-G POI Voltage (27.6-kV Side)	15.2	15.2	15.2	15.2	0	0	-5	0	0
	Voltage unbalanced (%) = 0								
L-L Voltage (370-V Side)	0.353	0.353	0.353	0.353	0	0	-5.1	0	0
	Voltage unbalanced (%) = 0								
	RMS Phase Magnitude			RMS Sequence Magnitude			Sequence Angle		
	(kA)	(kA)	(kA)	(kA)	(kA)	(kA)	(Degree)	(Degree)	(Degree)
Source to POI Current (27.6 kV Side)	0.059	0.059	0.059	0.059	0	0	-30.15	0	0
	Current unbalanced (%) = 0								
POI to Loads Current (27.6 kV Side)	0.059	0.059	0.059	0.059	0	0	-30	0	0
	Current unbalanced (%) = 0								
VSC to POI Current (27.6 kV Side)	0	0	0	0	0	0	0	0	0
VSC to POI Current (370 V Side)	0	0	0	0	0	0	0	0	0
VSC Power Output	Source to POI			POI to Loads			VSC to POI (27.6 kV side)		
	P	Q		P	Q		P	Q	
	(kW)	(kVar)		(kW)	(kVar)		(kW)	(kVar)	
	2450	1150		2450	1142		0	-8	

Table 3.8: Balanced RL load of 3 MVA (pf:0.9), Current-injection model (without LC filter) of VSC unit in service

Monitored Variable	RMS Phase Magnitude			RMS Sequence Magnitude			Sequence Angle		
	A	B	C	Positive	Negative	Zero	Positive	Negative	Zero
	(kV)	(kV)	(kV)	(kV)	(kV)	(kV)	(Degree)	(Degree)	(Degree)
L-G POI Voltage (27.6-kV Side)	15.29	15.29	15.29	15.29	0	0	-3.69	0	0
	Voltage unbalanced (%) = 0								
L-L Voltage (370-V Side)	0.355	0.355	0.355	0.355	0	0	-1.1	0	0
	Voltage unbalanced (%) = 0								
	RMS Phase Magnitude			RMS Sequence Magnitude			Sequence Angle		
	(kA)	(kA)	(kA)	(kA)	(kA)	(kA)	(Degree)	(Degree)	(Degree)
Source to POI Current (27.6 kV Side)	0.034	0.034	0.034	0.0343	0	0	-55.21	0	0
	Current unbalanced (%) = 0								
POI to Loads Current (27.6 kV Side)	0.0595	0.0595	0.0595	0.0596	0	0	-28.69	0	0
	Current unbalanced (%) = 0								
VSC to POI Current (27.6 kV Side)	0.033	0.033	0.033	0.033	0	0	-0.78	0	0
	Current unbalanced (%) = 0								
VSC to POI Current (370 V Side)	2.44	2.44	2.44	2.44	0	0	-31.1	0	0
	Current unbalanced (%) = 0								
VSC Power Output	Source to POI			POI to Loads			VSC to POI (27.6 kV side)		
	P	Q		P	Q		P	Q	
	(kW)	(kVar)		(kW)	(kVar)		(kW)	(kVar)	
	978	1232		2478	1155		1500	-76	

Table 3.9: Balanced RL load of 3 MVA (pf:0.9), Switched-model of VSC unit in service

Monitored Variable	RMS Phase Magnitude			RMS Sequence Magnitude			Sequence Angle		
	A	B	C	Positive	Negative	Zero	Positive	Negative	Zero
	(kV)	(kV)	(kV)	(kV)	(kV)	(kV)	(Degree)	(Degree)	(Degree)
L-G POI Voltage (27.6-kV Side)	15.3	15.3	15.3	15.3	0	0	-3.69	0	0
	Voltage unbalanced (%) = 0								
L-L Voltage (370-V Side)	0.355	0.355	0.355	0.355	0	0	-1.06	0	0
	Voltage unbalanced (%) = 0								
	RMS Phase Magnitude			RMS Sequence Magnitude			Sequence Angle		
	(kA)	(kA)	(kA)	(kA)	(kA)	(kA)	(Degree)	(Degree)	(Degree)
Source to POI Current (27.6 kV Side)	0.034	0.034	0.034	0.034	0	0	-55.65	0	0
	Current unbalanced (%) = 0								
POI to Loads Current (27.6 kV Side)	0.0596	0.0596	0.0597	0.0596	0	0	-28.69	0	0
	Current unbalanced (%) = 0								
VSC to POI Current (27.6 kV Side)	0.033	0.033	0.033	0.0329	0	0	-0.35	0	0
	Current unbalanced (%) = 0								
VSC to POI Current (370 V Side)	2.45	2.45	2.45	2.455	0	0	-32.2	0	0
	Current unbalanced (%) = 0								
VSC Power Output	Source to POI			POI to Loads			VSC to POI (27.6 kV side)		
	P	Q		P	Q		P	Q	
	(kW)	(kVar)		(kW)	(kVar)		(kW)	(kVar)	
	970	1201		2480	1156		1513	-45	

Case-1.4 : Unbalanced RL Load (2.15 MVA, 0.9 lagging power factor)

For this case, the total load of the feeder is adjusted to 2.15 MVA at 0.9 lagging power factor which corresponds to 1 MVA single-phase load (at phase A) and 1.15 MVA two-phase load connected to phases B and C.

The study results of Table 3.10 correspond to the unbalanced RL load of 2.15 MVA (0.9 lagging power factor) when the VSC unit is not in service. Due to unbalanced load, Table 3.10 shows that the degree of voltage imbalance at POI is 1.97%, and the degree of current imbalance (from source to POI) is 37.8%.

Table 3.11 shows the study results under the same unbalanced RL load when the VSC unit is in service, and represented by current-injection model (without LC filter), and injects 1.5 MW power in the system at POI. Table 3.11 indicates that the degree of voltage imbalance at POI is 1.96%. Despite of the presence of the VSC unit in the system, voltage results of Table 3.10 and 3.11 are practically the same. However, the degree of current imbalance (from source to POI) is increased from 37.8% (Table 3.10) to 61.36% (Table 3.11).

Table 3.12 presents the study results of the previous scenario under the same unbalanced RL load when the VSC unit is represented by the switched-model, and injects 1.5 MW power in the system at POI. A comparison of Table 3.11 and Table 3.12 shows that:

- The degree of voltage imbalance at POI changes from 1.96% (Table 3.11) to 1.97% (Table 3.12). The difference between the two tables is negligible, and thus the results are practically the same.
- The degrees of current imbalance (from source to POI) for both cases are practically the same.

Similar to the previous case studies, Table 3.11 and Table 3.12 conclude that the current-injection model is a valid representation of the VSC for the given scenario.

Table 3.10: Unbalanced RL load of 2.15 MVA (pf:0.9), VSC unit not in service

Monitored Variable	RMS Phase Magnitude			RMS Sequence Magnitude			Sequence Angle		
	A	B	C	Positive	Negative	Zero	Positive	Negative	Zero
	(kV)	(kV)	(kV)	(kV)	(kV)	(kV)	(Degree)	(Degree)	(Degree)
L-G POI Voltage (27.6-kV Side)	15.23	15.5	14.61	15.11	0.298	0.239	-5.3	79.8	-71.8
	Voltage unbalanced (%) = 1.97								
L-L Voltage (370-V Side)	0.352	0.356	0.345	0.351	0.0069	0	-5.41	79.73	0
	Voltage unbalanced (%) = 1.97								
	RMS Phase Magnitude			RMS Sequence Magnitude			Sequence Angle		
	(kA)	(kA)	(kA)	(kA)	(kA)	(kA)	(Degree)	(Degree)	(Degree)
Source to POI Current (27.6 kV Side)	0.053	0.064	0.101	0.0701	0.0265	0.009	-31.09	-174.48	18.22
	Current unbalanced (%) = 37.80								
POI to Loads Current (27.6 kV Side)	0.0593	0.0546	0.107	0.0701	0.0265	0.0196	-5.87	-148.1	51.87
	Current unbalanced (%) = 37.80								
VSC to POI Current (27.6 kV Side)	0.0114	0.0114	0.0111	0	0	0.0113	0	0	18.22
VSC to POI Current (370 V Side)	0	0	0	0	0	0	0	0	0
VSC Power Output	Source to POI			POI to Loads			VSC to POI (27.6 kV side)		
	P	Q		P	Q		P	Q	
	(kW)	(kVar)		(kW)	(kVar)		(kW)	(kVar)	
	2930	1456		2930	1447		0	-9	

Table 3.11: Unbalanced RL load of 2.15 MVA (pf:0.9), Current-injection model (without LC filter) of VSC unit in service

Monitored Variable	RMS Phase Magnitude			RMS Sequence Magnitude			Sequence Angle		
	A	B	C	Positive	Negative	Zero	Positive	Negative	Zero
	(kV)	(kV)	(kV)	(kV)	(kV)	(kV)	(Degree)	(Degree)	(Degree)
L-G POI Voltage (27.6-kV Side)	15.32	15.6	14.7	15.3	0.3	0.24	-4	81.1	-70.5
	Voltage unbalanced (%) = 1.96								
L-L Voltage (370-V Side)	0.354	0.358	0.346	0.352	0.007	0	-1.37	81.14	0
	Voltage unbalanced (%) = 1.99								
	RMS Phase Magnitude			RMS Sequence Magnitude			Sequence Angle		
	(kA)	(kA)	(kA)	(kA)	(kA)	(kA)	(Degree)	(Degree)	(Degree)
Source to POI Current (27.6 kV Side)	0.033	0.031	0.079	0.044	0.027	0.009	-50.37	-173.18	38.87
	Current unbalanced (%) = 61.36								
POI to Loads Current (27.6 kV Side)	0.06	0.055	0.108	0.0705	0.027	0.02	-29.6	-173.2	27.89
	Current unbalanced (%) = 38.30								
VSC to POI Current (27.6 kV Side)	0.044	0.025	0.033	0.033	0	0.0114	-1.06	0	19.5
	Current unbalanced (%) = 0								
VSC to POI Current (370 V Side)	2.46	2.46	2.46	2.46	0	0	-31.42	0	0
	Current unbalanced (%) = 0								
VSC Power Output	Source to POI			POI to Loads			VSC to POI (27.6 kV side)		
	P	Q		P	Q		P	Q	
	(kW)	(kVar)		(kW)	(kVar)		(kW)	(kVar)	
	1390	1490		2890	1420		1501	-77	

Table 3.12: Unbalanced RL load of 2.15 MVA (pf:0.9), Switched-model of VSC unit in service

Monitored Variable	RMS Phase Magnitude			RMS Sequence Magnitude			Sequence Angle		
	A	B	C	Positive	Negative	Zero	Positive	Negative	Zero
	(kV)	(kV)	(kV)	(kV)	(kV)	(kV)	(Degree)	(Degree)	(Degree)
L-G POI Voltage (27.6-kV Side)	15.34	15.61	14.71	15.22	0.3	0.24	-4.02	81.05	-70.53
	Voltage unbalanced (%) = 1.97								
L-L Voltage (370-V Side)	0.354	0.359	0.347	0.354	0.007	0	-1.37	80.8	0
	Voltage unbalanced (%) = 1.98								
	RMS Phase Magnitude			RMS Sequence Magnitude			Sequence Angle		
	(kA)	(kA)	(kA)	(kA)	(kA)	(kA)	(Degree)	(Degree)	(Degree)
Source to POI Current (27.6 kV Side)	0.0321	0.0313	0.0783	0.0436	0.0268	0.009	-49.58	-173.4	38.86
	Current unbalanced (%) = 61.47								
POI to Loads Current (27.6 kV Side)	0.0597	0.055	0.1079	0.0706	0.0267	0.0198	-29.67	-173.19	27.87
	Current unbalanced (%) = 37.82								
VSC to POI Current (27.6 kV Side)	0.0439	0.0248	0.0336	0.0329	0	0.0114	-2.88	0	19.51
	Current unbalanced (%) = 0								
VSC to POI Current (370 V Side)	2.471	2.46	2.462	2.46	0.007	0	-33	-78	0
	Current unbalanced (%) = 0.28								
VSC Power Output	Source to POI			POI to Loads			VSC to POI (27.6 kV side)		
	P	Q		P	Q		P	Q	
	(kW)	(kVar)		(kW)	(kVar)		(kW)	(kVar)	
	1390	1420		2900	1420		1512	2.8	

3.3.2 Case-2 : Short-Circuit Capacity of 16.6 MVA at POI

The main grid short-circuit MVA (SC_{MVA}) at the distribution substation is about 885 MVA. Due to the feeder impedance between the substation and POI, the SC_{MVA} at POI is 16.6 MVA. To reduce short-circuit MVA from 85 to 16.6 at POI, source impedance value is increased. Practically this can occur due to changes in the main grid configuration, e.g., when a transmission line is out of service.

Case-2.1 : Balanced RL Load (3 MVA, 0.9 lagging power factor)

Table 3.13 presents the study results under a balanced RL load of 3 MVA at 0.9 lagging power factor (downstream to POI) when the VSC unit is not in service. Table 3.13 demostrates, as expected, the three-phase voltages at POI are balanced.

Table 3.14 and Table 3.15 show the study results under the same balanced RL load of 3 MVA at 0.9 lagging power factor when the VSC unit is in service, and represented by the current-injection model (with LC filter) and the switched-model at POI, respectively. In both cases, the VSC injected power in the system is 1.5 MW. Table 3.14 and Table 3.15 indicate, as expected, the three-phase POI voltages remain balanced, and the two VSC unit models have the same behaviour for this scenario.

Table 3.13: Balanced RL load of 3 MVA (pf:0.9), VSC unit not in service

Monitored Variable	RMS Phase Magnitude			RMS Sequence Magnitude			Sequence Angle		
	A	B	C	Positive	Negative	Zero	Positive	Negative	Zero
	(kV)	(kV)	(kV)	(kV)	(kV)	(kV)	(Degree)	(Degree)	(Degree)
L-L POI Voltage (27.6-kV Side)	27.1	27.1	27.1	27.1	0.001	0	21.67	90.5	0
	Voltage unbalanced (%) = 0								
L-G POI Voltage (27.6-kV Side)	15.6	15.6	15.6	15.6	0.0006	0.0014	-8.32	137.6	37.1
	Voltage unbalanced (%) = 0								
L-L Voltage (370-V Side)	0.363	0.363	0.363	0.363	0	0	-8.32	0	0
	Voltage unbalanced (%) = 0								
	RMS Phase Magnitude			RMS Sequence Magnitude			Sequence Angle		
	(kA)	(kA)	(kA)	(kA)	(kA)	(kA)	(Degree)	(Degree)	(Degree)
Source to POI Current (27.6 kV Side)	0.061	0.061	0.061	0.061	0	0	-33.41	0	0
	Current unbalanced (%) = 0								
POI to Loads Current (27.6 kV Side)	0.061	0.061	0.061	0.061	0	0	-33.3	0	0
	Current unbalanced (%) = 0								
VSC to POI Current (27.6 kV Side)	0	0	0	0	0	0	0	0	0
VSC to POI Current (370 V Side)	0	0	0	0	0	0	0	0	0
VSC Power Output	Source to POI			POI to Loads			VSC to POI (27.6-kV side)		
	P	Q		P	Q		P	Q	
	(kW)	(kVar)		(kW)	(kVar)		(kW)	(kVar)	
	2594	1218		2594	1208		0	-9	

Table 3.14: Balanced RL load of 3 MVA (pf:0.9), Current-injection model (with LC filter) of VSC unit in service

Monitored Variable	RMS Phase Magnitude			RMS Sequence Magnitude			Sequence Angle		
	A	B	C	Positive	Negative	Zero	Positive	Negative	Zero
	(kV)	(kV)	(kV)	(kV)	(kV)	(kV)	(Degree)	(Degree)	(Degree)
L-L POI Voltage (27.6-kV Side)	29.1	29.1	29.1	29	0.001	0	25.5	93.4	0
	Voltage unbalanced (%) = 0								
L-G POI Voltage (27.6-kV Side)	16.8	16.8	16.8	16.8	0	0.001	-4.5	0	40.9
	Voltage unbalanced (%) = 0								
L-L Voltage (370-V Side)	0.392	0.392	0.392	0.392	0	0	-2.35	0	0
	Voltage unbalanced (%) = 0								
	RMS Phase Magnitude			RMS Sequence Magnitude			Sequence Angle		
	(kA)	(kA)	(kA)	(kA)	(kA)	(kA)	(Degree)	(Degree)	(Degree)
Source to POI Current (27.6 kV Side)	0.038	0.038	0.038	0.038	0	0	-43.88	0	0
	Current unbalanced (%) = 0								
POI to Loads Current (27.6 kV Side)	0.0653	0.0655	0.0655	0.0655	0	0	-29.4	0	0
	Current unbalanced (%) = 0								
VSC to POI Current (27.6 kV Side)	0.03	0.03	0.03	0.03	0	0	-11.17	0	0
	Current unbalanced (%) = 0								
VSC to POI Current (370 V Side)	2.25	2.25	2.25	2.25	0	0	-41.5	0	0
	Current unbalanced (%) = 0								
VSC Power Output	Source to POI			POI to Loads			VSC to POI (27.6-kV side)		
	P	Q		P	Q		P	Q	
	(kW)	(kVar)		(kW)	(kVar)		(kW)	(kVar)	
	1480	1216		2987	1391		1506	175	

Table 3.15: Balanced RL load of 3 MVA (pf:0.9), Switched-model of VSC unit in service

Monitored Variable	RMS Phase magnitude			RMS Sequence magnitude			Sequence Angle		
	A	B	C	Positive	Negative	Zero	Positive	Negative	Zero
	(kV)	(kV)	(kV)	(kV)	(kV)	(kV)	(Degree)	(Degree)	(Degree)
L-L POI Voltage (27.6-kV Side)	27.4	27.4	27.4	27.4	0.007	0	26.6	-164	0
	Voltage unbalanced (%) = 0.03								
L-G POI Voltage (27.6-kV Side)	15.8	15.8	15.8	15.8	0.005	0.001	-3.4	-51	42
	Voltage unbalanced (%) = 0.03								
L-L Voltage (370-V Side)	0.366	0.366	0.366	0.366	0	0	-0.92	0	0
	Voltage unbalanced (%) = 0								
	RMS Phase magnitude			RMS Sequence magnitude			Sequence Angle		
	(kA)	(kA)	(kA)	(kA)	(kA)	(kA)	(Degree)	(Degree)	(Degree)
Source to POI Current (27.6 kV Side)	0.037	0.037	0.037	0.037	0	0	-52.8	0	0
	Current unbalanced (%) = 0								
POI to Loads Current (27.6 kV Side)	0.062	0.062	0.062	0.062	0	0	-28.4	0	0
	Current unbalanced (%) = 0								
VSC to POI Current (27.6 kV Side)	0.032	0.032	0.032	0.032	0	0	0.78	0	0
	Current unbalanced (%) = 0								
VSC to POI Current (370 V Side)	2.37	2.37	2.37	2.37	0	0	-29.7	0	0
	Current unbalanced (%) = 0								
VSC Power Output	Source to POI			POI to Loads			VSC to POI (27.6-kV side)		
	P	Q		P	Q		P	Q	
	(kW)	(kVar)		(kW)	(kVar)		(kW)	(kVar)	
	1146	1340		2650	1235		1504	-105	

Case-2.2 : Unbalanced RL Load (2.15 MVA, 0.9 lagging power factor)

For this case, the same unbalanced load scenario of Case-1, Section 3.3.1, page 17 is used.

Table 3.16 presents the study results under unbalanced RL load of 2.15 MVA at 0.9 lagging power factor when the VSC unit is not in service. Due to the unbalanced load, Table 3.16 indicates that the degree of the voltage imbalance at POI is 2.15%, and the degree of current imbalance (from source to POI) is 14.29%.

Table 3.17 shows the study results under the same unbalanced RL load when the VSC unit, which is represented by the current-injection model (with LC filter), is in service and injects 1.5 MW power in the system at POI. Table 3.17 demonstrates that the degree of voltage imbalance at POI is 2.17%. Although the VSC unit is in service, the voltage imbalance results of the Table 3.16 and 3.17 are practically the same. However, the degree of current imbalance (from source to POI) is increased from 14.29% (Table 3.16) to 32.61% (Table 3.17). The reason is the same as explained for Case-1, Section 3.3.1, page 28.

Table 3.18 presents the study results under the same unbalanced load when the VSC unit is represented by the switched-model, and injects 1.5 MW power in the system at POI. Comparing the results of Table 3.17 and 3.18 indicates :

- The degrees of voltage imbalance at POI change from 2.17% (Table 3.17) to 2.16% (Table 3.18). The results, as presented, are practically the same.
- The degrees of current imbalance (from source to POI) change from 32.61% (Table 3.17) to 28.09% (Table 3.18). The results conclude that the current-injection model increases the degree of current imbalance as compared with the switched-model. The reason is that the fixed impedance model are used to present the loads, and for each model of converter are connected at POI, the voltage at POI changes. Therefore, the current (from source to POI) is altered, and accordingly the degree of current imbalance changes.

Table 3.16 to Table 3.18 conclude that both models of the VSC unit, subject to unbalanced RL load scenario, produce noteably different results and may not be used interchangeably.

Table 3.16: Unbalanced RL load of 2.15 MVA (pf:0.9), VSC unit not in service

Monitored Variable	RMS Phase magnitude			RMS Sequence magnitude			Sequence Angle		
	A	B	C	Positive	Negative	Zero	Positive	Negative	Zero
	(kV)	(kV)	(kV)	(kV)	(kV)	(kV)	(Degree)	(Degree)	(Degree)
L-L POI Voltage (27.6-kV Side)	27.3	27.4	28.3	27.7	0.595	0	23.4	-100	0
	Voltage unbalanced (%) = 2.15								
L-G POI Voltage (27.6-kV Side)	16.5	15.4	16	15.98	0.344	0.387	-6.6	-70	-3.4
	Voltage unbalanced (%) = 2.15								
L-L Voltage (370-V Side)	0.374	0.363	0.376	0.371	0.008	0	-6.6	-71	0
	Voltage unbalanced (%) = 2.16								
	RMS Phase magnitude			RMS Sequence magnitude			Sequence Angle		
	(kA)	(kA)	(kA)	(kA)	(kA)	(kA)	(Degree)	(Degree)	(Degree)
Source to POI Current (27.6 kV Side)	0.052	0.052	0.044	0.049	0.007	0.003	-32	30	91
	Current unbalanced (%) = 14.29								
POI to Loads Current (27.6 kV Side)	0.049	0.047	0.062	0.049	0.007	0.021	-32	24	87
	Current unbalanced (%) = 14.29								
VSC to POI Current (27.6 kV Side)	0.0185	0.0182	0.0182	0	0	0.0183	0	0	86.7
VSC to POI Current (370 V Side)	0	0	0	0	0	0	0	0	0
VSC Power Output	Source to POI			POI to Loads			VSC to POI (27.6-kV side)		
	P	Q		P	Q		P	Q	
	(kW)	(kVar)		(kW)	(kVar)		(kW)	(kVar)	
	2110	1020		2110	1010		0	-10	

Table 3.17: Unbalanced RL load of 2.15 MVA (pf:0.9), Current-injection model (with LC filter) of VSC unit in service

Monitored Variable	RMS Phase magnitude			RMS Sequence magnitude			Sequence Angle		
	A	B	C	Positive	Negative	Zero	Positive	Negative	Zero
	(kV)	(kV)	(kV)	(kV)	(kV)	(kV)	(Degree)	(Degree)	(Degree)
L-L POI Voltage (27.6-kV Side)	27.98	28.06	28.93	28.31	0.615	0	28	-96.4	0
	Voltage unbalanced (%) = 2.17								
L-G POI Voltage (27.6-kV Side)	16.9	15.78	16.37	16.35	0.355	0.397	-1.99	-66.5	1.27
	Voltage unbalanced (%) = 2.17								
L-L Voltage (370-V Side)	0.385	0.373	0.387	0.382	0.008	0	0.272	-66.4	0
	Voltage unbalanced (%) = 2.09								
	RMS Phase magnitude			RMS Sequence magnitude			Sequence Angle		
	(kA)	(kA)	(kA)	(kA)	(kA)	(kA)	(Degree)	(Degree)	(Degree)
Source to POI Current (27.6 kV Side)	0.023	0.03	0.018	0.023	0.0075	0.0027	-53.5	28.45	95.6
	Current unbalanced (%) = 32.61								
POI to Loads Current (27.6 kV Side)	0.05	0.049	0.064	0.0498	0.007	0.0215	-27.39	28.5	91.84
	Current unbalanced (%) = 14.06								
VSC to POI Current (27.6 kV Side)	0.033	0.02	0.049	0.031	0	0.0187	-8.24	0	91.3
	Current unbalanced (%) = 0								
VSC to POI Current (370 V Side)	2.306	2.301	2.31	2.306	0.005	0	-38.6	-126.4	0
	Current unbalanced (%) = 0.22								
VSC Power Output	Source to POI			POI to Loads			VSC to POI (27.6-kV side)		
	P	Q		P	Q		P	Q	
	(kW)	(kVar)		(kW)	(kVar)		(kW)	(kVar)	
	703	900		2206	1055		1505	165	

Table 3.18: Unbalanced RL load of 2.15 MVA (pf:0.9), Switched-model of VSC unit in service

Monitored Variable	RMS Phase magnitude			RMS Sequence magnitude			Sequence Angle		
	A	B	C	Positive	Negative	Zero	Positive	Negative	Zero
	(kV)	(kV)	(kV)	(kV)	(kV)	(kV)	(Degree)	(Degree)	(Degree)
L-L POI Voltage (27.6-kV Side)	27.57	27.65	28.51	27.9	0.604	0	28.2	-97.6	0
	Voltage unbalanced (%) = 2.16								
L-G POI Voltage (27.6-kV Side)	16.64	15.56	16.14	16.11	0.348	0.391	-1.744	-66.68	1.47
	Voltage unbalanced (%) = 2.16								
L-L Voltage (370-V Side)	0.376	0.365	0.378	0.374	0.008	0	0.607	-68.2	0
	Voltage unbalanced (%) = 2.14								
	RMS Phase magnitude			RMS Sequence magnitude			Sequence Angle		
	(kA)	(kA)	(kA)	(kA)	(kA)	(kA)	(Degree)	(Degree)	(Degree)
Source to POI Current (27.6 kV Side)	0.026	0.034	0.023	0.0267	0.0075	0.0027	-62	27	96
	Current unbalanced (%) = 28.09								
POI to Loads Current (27.6 kV Side)	0.049	0.048	0.063	0.0491	0.007	0.0211	-27.39	28.9	92.1
	Current unbalanced (%) = 14.26								
VSC to POI Current (27.6 kV Side)	0.036	0.018	0.048	0.031	0	0.0184	2.15	0	91.3
	Current unbalanced (%) = 0								
VSC to POI Current (370 V Side)	2.32	2.35	2.35	2.328	0.01	0	-28.3	-155.56	0
	Current unbalanced (%) = 0.43								
VSC Power Output	Source to POI			POI to Loads			VSC to POI (27.6-kV side)		
	P	Q		P	Q		P	Q	
	(kW)	(kVar)		(kW)	(kVar)		(kW)	(kVar)	
	625	1114		2130	1002		1505	-103	

3.3.3 Case-3 : Short-Circuit Capacity of 8.5 MVA at POI

The same method of Section 3.3.2 is used to change POI SC_{MVA} from 85 to 8.5. The same scenarios of Section 3.3.2 are also applied in this section to investigate voltage and current imbalance under the two models of the VSC.

Case-3.1 : Balanced RL Load (3 MVA, 0.9 lagging power factor)

Table 3.19 shows the study results under the balanced RL load of 3 MVA at 0.9 lagging power factor when the VSC unit is not in service. Table 3.19 exhibits, as expected, that the three-phase POI voltage is balanced. Table 3.20 and 3.21 show the study results under the same balanced RL load when the VSC unit is in service, and represented by the current-injection model (with LC filter) and the switched-model, respectively, and injects 1.5 MW power in the system at POI. As anticipated, Table 3.19 to Table 3.21 indicate that both models of the VSC unit provide identical responses under balanced conditions.

Table 3.19: Balanced RL load of 3 MVA (pf:0.9), VSC unit not in service

Monitored Variable	RMS Phase magnitude			RMS Sequence magnitude			Sequence Angle		
	A	B	C	Positive	Negative	Zero	Positive	Negative	Zero
	(kV)	(kV)	(kV)	(kV)	(kV)	(kV)	(Degree)	(Degree)	(Degree)
L-L POI Voltage (27.6-kV Side)	27.5	27.5	27.5	27.5	0.002	0	11.96	72.69	0
	Voltage unbalanced (%) = 0.01								
L-G POI Voltage (27.6-kV Side)	15.9	15.9	15.9	15.85	0.001	0.0014	-18.32	111	27.1
	Voltage unbalanced (%) = 0.01								
L-L Voltage (370-V Side)	0.368	0.368	0.368	0.368	0	0	-18.04	0	0
	Voltage unbalanced (%) = 0								
	RMS Phase magnitude			RMS Sequence magnitude			Sequence Angle		
	(kA)	(kA)	(kA)	(kA)	(kA)	(kA)	(Degree)	(Degree)	(Degree)
Source to POI Current (27.6 kV Side)	0.062	0.062	0.062	0.062	0	0	-43.7	0	0
	Current unbalanced (%) = 0								
POI to Loads Current (27.6 kV Side)	0.062	0.062	0.062	0.062	0	0	-43.1	0	0
	Current unbalanced (%) = 0								
VSC to POI Current (27.6 kV Side)	0	0	0	0	0	0	0	0	0
VSC to POI Current (370 V Side)	0	0	0	0	0	0	0	0	0
VSC Power Output	Source to POI			POI to Loads			VSC to POI (27.6-kV side)		
	P	Q		P	Q		P	Q	
	(kW)	(kVar)		(kW)	(kVar)		(kW)	(kVar)	
	2668	1251		2668	1242		0	-10	

Table 3.20: Balanced RL load of 3 MVA (pf:0.9), Current-injection model (with LC filter) of VSC unit in service

Monitored Variable	RMS Phase magnitude			RMS Sequence magnitude			Sequence Angle		
	A	B	C	Positive	Negative	Zero	Positive	Negative	Zero
	(kV)	(kV)	(kV)	(kV)	(kV)	(kV)	(Degree)	(Degree)	(Degree)
L-L POI Voltage (27.6-kV Side)	29.4	29.4	29.4	29.37	0.002	0	20.53	80.89	0
	Voltage unbalanced (%) = 0.01								
L-G POI Voltage (27.6-kV Side)	16.96	16.96	16.96	16.96	0.001	0.0017	-9.5	119	35.6
	Voltage unbalanced (%) = 0.01								
L-L Voltage (370-V Side)	0.396	0.396	0.396	0.395	0	0	-7.4	0	0
	Voltage unbalanced (%) = 0								
	RMS Phase magnitude			RMS Sequence magnitude			Sequence Angle		
	(kA)	(kA)	(kA)	(kA)	(kA)	(kA)	(Degree)	(Degree)	(Degree)
Source to POI Current (27.6 kV Side)	0.039	0.039	0.039	0.039	0	0	-48.22	0	0
	Current unbalanced (%) = 0								
POI to Loads Current (27.6 kV Side)	0.066	0.066	0.066	0.066	0	0	-34.44	0	0
	Current unbalanced (%) = 0								
VSC to POI Current (27.6 kV Side)	0.03	0.03	0.03	0.0298	0	0	-16.3	0	0
	Current unbalanced (%) = 0								
VSC to POI Current (370 V Side)	2.23	2.23	2.23	2.23	0	0	-46.69	0	0
	Current unbalanced (%) = 0								
VSC Power Output	Source to POI			POI to Loads			VSC to POI (27.6-kV side)		
	P	Q		P	Q		P	Q	
	(kW)	(kVar)		(kW)	(kVar)		(kW)	(kVar)	
	1544	1241		3051	1421		1507	182	

Table 3.21: Balanced RL load of 3 MVA (pf:0.9), Switched-model of VSC unit in service

Monitored Variable	RMS Phase magnitude			RMS Sequence magnitude			Sequence Angle		
	A	B	C	Positive	Negative	Zero	Positive	Negative	Zero
	(kV)	(kV)	(kV)	(kV)	(kV)	(kV)	(Degree)	(Degree)	(Degree)
L-L POI Voltage (27.6-kV Side)	28.59	28.57	28.55	28.57	0.029	0	21.4	55.8	0
	Voltage unbalanced (%) = 0.10								
L-G POI Voltage (27.6-kV Side)	16.48	16.48	16.48	16.49	0.006	0.0016	-8.57	101.7	36.5
	Voltage unbalanced (%) = 0.04								
L-L Voltage (370-V Side)	0.382	0.382	0.382	0.382	0	0	-6.28	0	0
	Voltage unbalanced (%) = 0								
	RMS Phase magnitude			RMS Sequence magnitude			Sequence Angle		
	(kA)	(kA)	(kA)	(kA)	(kA)	(kA)	(Degree)	(Degree)	(Degree)
Source to POI Current (27.6 kV Side)	0.04	0.04	0.04	0.04	0	0	-54.8	0	0
	Current unbalanced (%) = 0								
POI to Loads Current (27.6 kV Side)	0.064	0.064	0.064	0.064	0	0	-33.5	0	0
	Current unbalanced (%) = 0								
VSC to POI Current (27.6 kV Side)	0.03	0.03	0.03	0.0305	0	0	-4.7	0	0
	Current unbalanced (%) = 0								
VSC to POI Current (370 V Side)	2.27	2.27	2.26	2.28	0.002	0	-46.69	0	0
	Current unbalanced (%) = 0.09								
VSC Power Output	Source to POI			POI to Loads			VSC to POI (27.6-kV side)		
	P	Q		P	Q		P	Q	
	(kW)	(kVar)		(kW)	(kVar)		(kW)	(kVar)	
	1377	1439		2884	1343		1503	-96	

Case-3.2 : Unbalanced RL Load (2.15 MVA, 0.9 lagging power factor)

For this case, the unbalanced load of the feeder is adjusted to 2.15 MVA at 0.9 lagging power factor similar to that of Case-1, Section 3.3.1, page 17. Table 3.22 introduces the study results under unbalanced load of 2.15 MVA at 0.9 lagging power factor when the VSC unit is not in service. Table 3.22 shows that the degree of voltage imbalance at POI is 2.17%, and the degree of current imbalance (from source to POI) is 6.12%.

Table 3.23 shows the study results under the same unbalanced RL load when VSC unit is represented by the current-injection model (with LC filter), and injects 1.5 MW power in the system at POI. Table 3.23 shows that the degree of the voltage imbalance at POI is 2.21%. In spite of the presence of the VSC unit, the POI voltage imbalance of Table 3.22 and 3.23 are practically the same. However, the degree of current imbalance (from source to POI) is increased from 6.12% (Table 3.22) to 15.79% (Table 3.23).The reason is the same as explained for Case-1, Section 3.3.1, page 28.

Table 3.24 shows the study results under the same unbalanced RL load when the VSC unit is represented by the switched-model, and injects 1.5 MW power in the system at POI. The comparison of Table 3.23 and 3,24 indicates that:

- The degrees of voltage imbalance at POI changes from 2.21% (Table 3.23) to 2.18% (Table 3.24) which are practically the same.
- The degrees of current imbalance (from source to POI) change from 15.79% (Table 3.23) to 13.5% (Table 3.24). The current-injection model of the VSC unit results in a higher level of negative sequence current as compared with the switched-model of the VSC unit. The reason is the same as explained in Section 3.3.2, page 36.

The results of Table 3.22, 3.23 and 3.24 conclude that the two models of the VSC unit generate different results however the differences are not significant.

Table 3.22: Unbalanced RL load of 2.15 MVA (pf:0.9), VSC unit not in service

Monitored Variable	RMS Phase magnitude			RMS Sequence magnitude			Sequence Angle		
	A	B	C	Positive	Negative	Zero	Positive	Negative	Zero
	(kV)	(kV)	(kV)	(kV)	(kV)	(kV)	(Degree)	(Degree)	(Degree)
L-L POI Voltage (27.6-kV Side)	27.45	27.41	28.33	27.7	0.6	0	16.22	-101	0
	Voltage unbalanced (%) = 2.17								
L-G POI Voltage (27.6-kV Side)	16.62	15.43	15.99	16	0.35	0.42	-13.8	-71.5	-10.13
	Voltage unbalanced (%) = 2.19								
L-L Voltage (370-V Side)	0.376	0.363	0.375	0.371	0.008	0	-13.77	-71.45	0
	Voltage unbalanced (%) = 2.16								
	RMS Phase magnitude			RMS Sequence magnitude			Sequence Angle		
	(kA)	(kA)	(kA)	(kA)	(kA)	(kA)	(Degree)	(Degree)	(Degree)
Source to POI Current (27.6 kV Side)	0.046	0.046	0.043	0.049	0.003	0.001	-32	30	91
	Current unbalanced (%) = 6.12								
POI to Loads Current (27.6 kV Side)	0.042	0.041	0.062	0.044	0.003	0.021	-32	24	87
	Current unbalanced (%) = 6.82								
VSC to POI Current (27.6 kV Side)	0.02	0.02	0.02	0	0	0.0183	0	0	86.7
VSC to POI Current (370 V Side)	0	0	0	0	0	0	0	0	0
VSC Power Output	Source to POI			POI to Loads			VSC to POI (27.6-kV side)		
	P	Q		P	Q		P	Q	
	(kW)	(kVar)		(kW)	(kVar)		(kW)	(kVar)	
	1931	893		1932	885		1	-10	

Table 3.23: Unbalanced RL load of 2.15 MVA (pf:0.9), Current-injection model (with LC filter) of VSC unit in service

Monitored Variable	RMS Phase magnitude			RMS Sequence magnitude			Sequence Angle		
	A	B	C	Positive	Negative	Zero	Positive	Negative	Zero
	(kV)	(kV)	(kV)	(kV)	(kV)	(kV)	(Degree)	(Degree)	(Degree)
L-L POI Voltage (27.6-kV Side)	29.06	29.1	30.06	29.4	0.65	0	25.7	-92	0
	Voltage unbalanced (%) = 2.21								
L-G POI Voltage (27.6-kV Side)	17.62	16.36	16.96	16.98	0.37	0.44	-1.99	-66.5	1.27
	Voltage unbalanced (%) = 2.18								
L-L Voltage (370-V Side)	0.401	0.387	0.4	0.396	0.0088	0	0.272	-66.4	0
	Voltage unbalanced (%) = 2.22								
	RMS Phase magnitude			RMS Sequence magnitude			Sequence Angle		
	(kA)	(kA)	(kA)	(kA)	(kA)	(kA)	(Degree)	(Degree)	(Degree)
Source to POI Current (27.6 kV Side)	0.0205	0.0237	0.019	0.0209	0.0033	0.0012	-54.8	30.87	92.1
	Current unbalanced (%) = 15.79								
POI to Loads Current (27.6 kV Side)	0.044	0.043	0.066	0.047	0.0032	0.022	-28.9	30.94	89.5
	Current unbalanced (%) = 6.81								
VSC to POI Current (27.6 kV Side)	0.033	0.019	0.05	0.03	0	0.021	-11.1	0	89.39
	Current unbalanced (%) = 0								
VSC to POI Current (370 V Side)	2.225	2.219	2.228	2.223	0.005	0	-41.5	-122.3	0
	Current unbalanced (%) = 0.22								
VSC Power Output	Source to POI			POI to Loads			VSC to POI (27.6-kV side)		
	P	Q		P	Q		P	Q	
	(kW)	(kVar)		(kW)	(kVar)		(kW)	(kVar)	
	667	815		2171	995		1505	180	

Table 3.24: Unbalanced RL load of 2.15 MVA (pf:0.9), Switched-model of VSC unit in service

Monitored Variable	RMS Phase magnitude			RMS Sequence magnitude			Sequence Angle		
	A	B	C	Positive	Negative	Zero	Positive	Negative	Zero
	(kV)	(kV)	(kV)	(kV)	(kV)	(kV)	(Degree)	(Degree)	(Degree)
L-L POI Voltage (27.6-kV Side)	28.18	28.2	29.11	28.49	0.62	0	25.7	-92	0
	Voltage unbalanced (%) = 2.18								
L-G POI Voltage (27.6-kV Side)	17.06	15.85	16.44	16.35	0.355	0.43	-1.99	-66.5	1.27
	Voltage unbalanced (%) = 2.17								
L-L Voltage (370-V Side)	0.385	0.373	0.386	0.382	0.0085	0	0.272	-66.4	0
	Voltage unbalanced (%) = 2.23								
	RMS Phase magnitude			RMS Sequence magnitude			Sequence Angle		
	(kA)	(kA)	(kA)	(kA)	(kA)	(kA)	(Degree)	(Degree)	(Degree)
Source to POI Current (27.6 kV Side)	0.0227	0.0267	0.022	0.0237	0.0032	0.0012	-65.9	30.6	92.1
	Current unbalanced (%) = 13.50								
POI to Loads Current (27.6 kV Side)	0.043	0.042	0.064	0.0457	0.0031	0.022	-28.1	32.8	90.34
	Current unbalanced (%) = 6.78								
VSC to POI Current (27.6 kV Side)	0.037	0.017	0.049	0.031	0	0.02	0.11	0	90.25
	Current unbalanced (%) = 0								
VSC to POI Current (370 V Side)	2.27	2.28	2.292	2.278	0.011	0	-30.13	-160.46	0
	Current unbalanced (%) = 0.48								
VSC Power Output	Source to POI			POI to Loads			VSC to POI (27.6-kV side)		
	P	Q		P	Q		P	Q	
	(kW)	(kVar)		(kW)	(kVar)		(kW)	(kVar)	
	541	1029		2043	932		1505	-91	

3.3.4 Case-4 : Short-Circuit Capacity of Less Than 8.5 MVA at POI

The Short-circuit ratio (SCR) of buses, at the transmission voltage levels, practically can be as low as unity (or even less). However, in distribution systems the SCR value is often larger than unity. For example, for the reported case studies of Section 3.3.1 to Section 3.3.3, the SCR value changes from $85/1.5 = 56.66$ to $8.5/1.5 = 5.66$.

For urban distribution feeders, the SCR value at different buses on the feeder is often significantly higher than 5 and thus one can conclude that the switched-model and current-injection model of the VSC provide (practically) identical results. However, the rural distribution feeders are (i) significantly longer (up to even 60-km) than urban feeders, and (ii) supply highly sparse loads and thus the conductors have higher impedances. Thus the SC_{MVA} at buses close to the end of the feeder can be fairly low and as a result the SCR value can be less than 5.

To compare the effects of the two VSC models on the POI voltage imbalance, three different values of SCR, i.e., $6/1.5 = 4$, $4.5/1.5 = 3$ and $2.25/1.5 = 1.5$ are considered and the results are as follows.

Case-4.1 : Unbalanced RL Load (2.15 MVA, 0.9 lagging power factor, SCR = 4)

For this scenario, the degree of POI voltage imbalance for the switched-model (current-injection model) are 2.34 (2.24), 2.28 (2.23) and 2.39 (2.21). The reason for the noticeable difference between the corresponding results is that the injected current harmonic in the system by the switched-model distorts the POI voltages.

Case-4.2 : Unbalanced RL Load (2.15 MVA, 0.9 lagging power factor, SCR = 3)

In this case, the degree of POI voltage imbalance for the switched-model (current-injection model) are 3.18 (2.32), 3.41 (2.18) and 2.82 (2.26). There are two factors which contribute to the higher degree of voltage imbalance of the switched-model, i.e., distortion due to harmonics and negative-sequence component. The fidelity of the PLL used by the VSC for synchronization, i.e., the extend that the PLL is immune to the effect of negative-sequence voltage component and harmonics becomes a main consideration in this regard.

In practice, as of now, there is no specific standard/requirements on the PLL specifications. Therefore, although the injection-model results are "better" than the switched-model, they are pessimistic and can be misleading. Therefore, the injection-model is not recommended for SCR = 3.

Case-4.3 : Unbalanced RL Load (2.15 MVA, 0.9 lagging power factor, SCR = 1.5)

For this scenario, the switched-model fails. The reason is that the PLL cannot handle the harmonic distortion and cannot synchronize the VSC to the system. The injection-model, however, provide voltage imbalance degrees of 2.35, 2.62, and 2.28 at POI. It should be noted that the switched-model results (failure to operate) is potentially more realistic than those of the injection-model.

3.4 Conclusions

This chapter provided a comprehensive steady-state performance calculation of the behaviour of a VSC-interfaced distributed resource unit under different SCR values and unbalanced conditions of the host distribution system. The switched-model of the VSC is used as the benchmark (reference) model for evaluation of the results obtained from current-injection (or current-sourced) model.

The study results show that:

- When the SCR at the point of interconnection (POI) of the VSC unit is larger than 5, i.e., short-circuit capacity of the system is larger than 8.5-MVA, and the POI voltage imbalance within 2%, the current-injection model reproduces the same results (at the fundamental frequency) as those of the switched-model. Thus the two models can be used interchangeably.

- Under the above conditions, the presence of VSC unit can result in the high (67%) current unbalance, upstream to POI, which can violate the acceptable limits. However, this is a bi-product of the VSC-interfaced power generation property and not the model used to represent the VSC.

- When the SCR at POI becomes less than 5 and the voltage imbalance is within 2%, the difference between the corresponding results of the two VSC models become noticeable. The main reason is the impact of harmonics generated by the switched-model and the POI negative-sequence voltage on the behaviour of the VSC PLL. Since the current-injection does not generate harmonics, the corresponding PLL behaves "better". Thus, the results from the current-injection model are optimistic and necessarily not reliable.

- At very low SCR values, e.g., SCR ≤ 2, the switched-model fails to operate. This is due to inability of the PLL to provide proper synchronization. However, the current-injection model can provide synchronization. The inability of the VSC switched-model to operate is more realistic and the results from the VSC current-injection model are not acceptable.

Table 3.25: Summary of Steady-state Results

DG unit		NO DG unit		Current-Injection Model		Switched-model	
POI SCMVA (SCR)	LOAD TYPES	Voltage Imbalance (%)	Current Imbalance (%)	Voltage Imbalance (%)	Current Imbalance (%)	Voltage Imbalance (%)	Current Imbalance (%)
85.0 (56.6)	R	1.91	37.06	1.91	67.52	1.93	68.48
	RL	1.97	37.8	1.96	61.36	1.97	61.47
16.6 (11.1)	RL	2.15	14.29	2.17	32.61	2.16	28.1
8.5 (5.6)	RL	2.17	6.12	2.21	15.79	2.18	13.5
6.0 (4)	RL	-	-	2.21	-	2.39	-
4.5 (3)	RL	-	-	2.32	-	3.18	-
2.25 (1.5)	RL	-	-	2.35	-	fails	-

Chapter 4

Transient Responses of VSC Models

4.1 Introduction

Chapter 3 investigated the steady-state behaviour of the switched-model and the current-injection model of a three-phase VSC-interfaced distributed resource, under balanced and unbalanced conditions. The main objective of this chapter is to evaluate and compare the corresponding responses of the two models during and subsequent to the system transients, e.g., faults. The same study system of chapter 3 is used in this chapter. The VSC unit is the 1.5 MW, 370 V system that was also presented in Chapter 2 and Chapter 3. The reported studies in this chapter are based on time-domain simulation studies of the study system in the PSCAD/EMTDC platform.

4.2 Case Studies

The reported studies are for the case that (i) the load is a balanced RL at 0.9 lagging power factor, (ii) the POI short-circuit capacity is 16.6 MVA, (iii) the VSC injects 1.5 MW into the system, (iv) the bus voltage of the study system are within 0.95 to 1.05 per unit. The transient in the system are due to faults which are occurred the same location that is bus B11 of Figure 3.1. The imbalance in the system is due to asymmetrical faults, e.g., LG faults. Four different fault conditions were investigated, i.e.,

- line-to-line-to-line (LLL) fault, with the fault impedance of 0.01 ohm,
- line-to-line-to-ground (LLG) fault, with the fault impedance of 0.01 ohm,
- line-to-ground (LG) fault, with the fault impedance of 0.01 ohm,
- line-to-line (LL) fault, with the fault impedance of 0.01 ohm.

Each fault is imposed at time t = 0.1 s and self-cleared at time t = 0.25 s at the first current zero-crossing for each phase.

4.2.1 LLL Fault

Figures 4.1 and 4.2 show the voltage and current waveforms respectively, for pre-fault, fault and post-fault periods when the VSC is represented by the current-injection model. Figures 4.3 and 4.4 show the voltage and current waveforms when the VSC is represented by the switched-model.

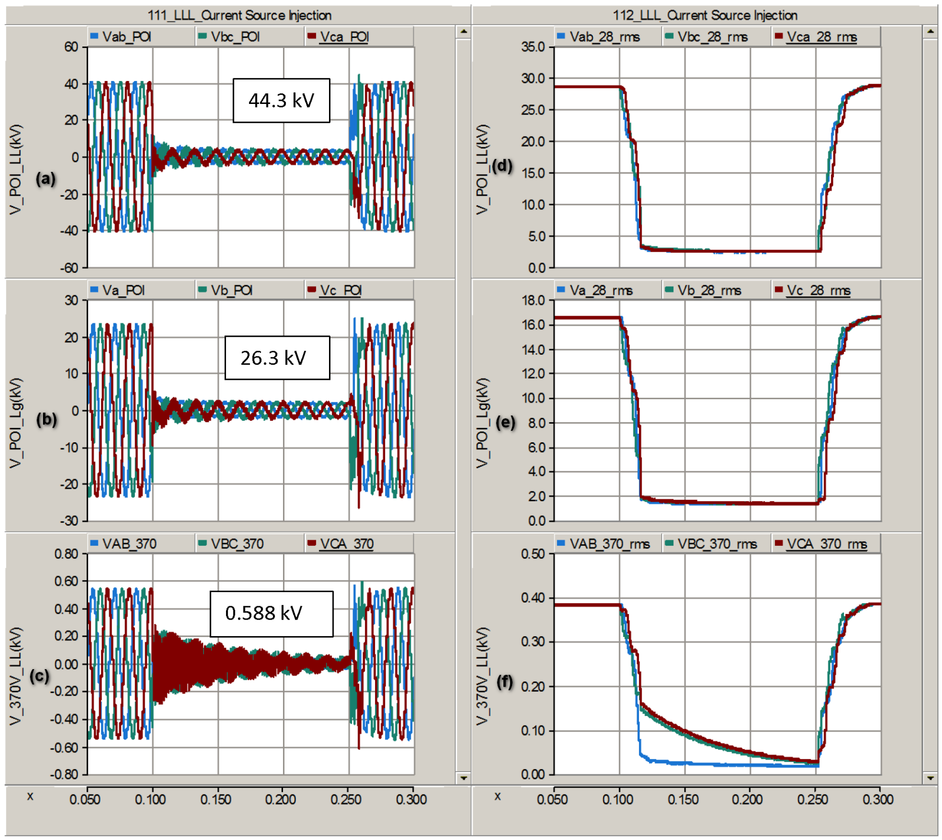

Figure 4.1: LLL fault, Current-Injection Model

(a) POI instantaneous line-to-line voltages

(b) POI instantaneous line-to-ground voltages

(c) 370-V side instantaneous line-to-line voltages

(d) POI rms line-to-line voltages

(e) POI rms line-to-ground voltages

(f) 370 V side rms line-to-line voltages

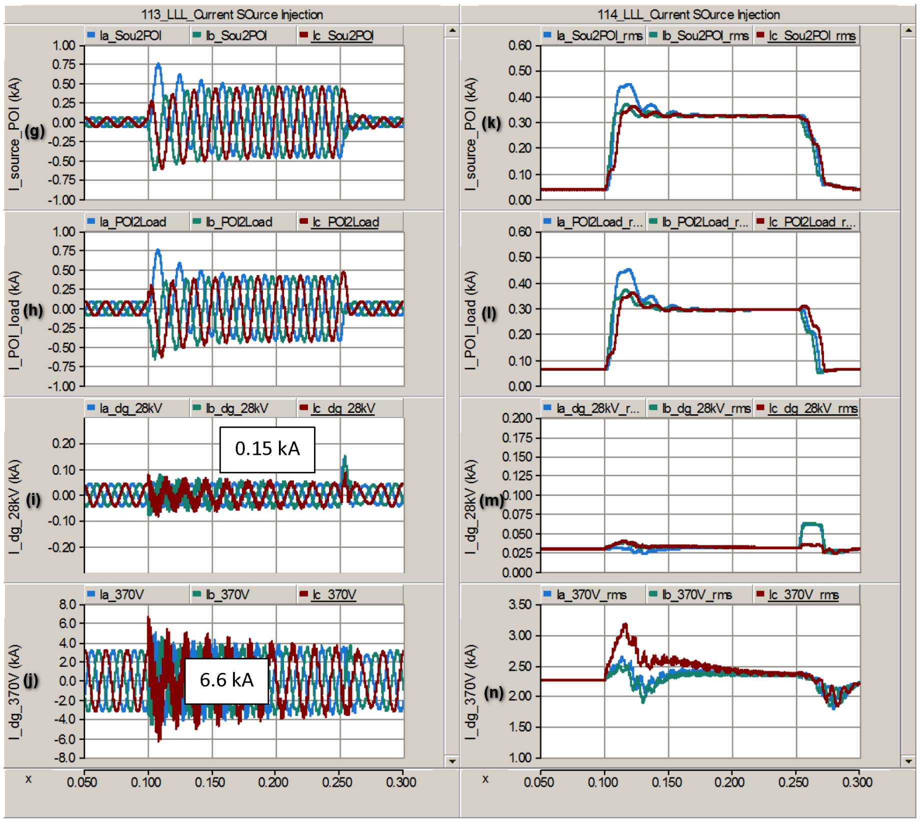

Figure 4.2: LLL fault, Current-Injection Model

(g) Source to POI instantaneous currents

(h) POI to load instantaneous currents

(i) VSC 27.6 kV side instantaneous currents

(j) VSC 370 V side instantaneous currents

(k) Source to POI rms currents

(l) POI to load rms currents

(m) VSC 27.6 kV side rms currents

(n) VSC 370 V side rms currents

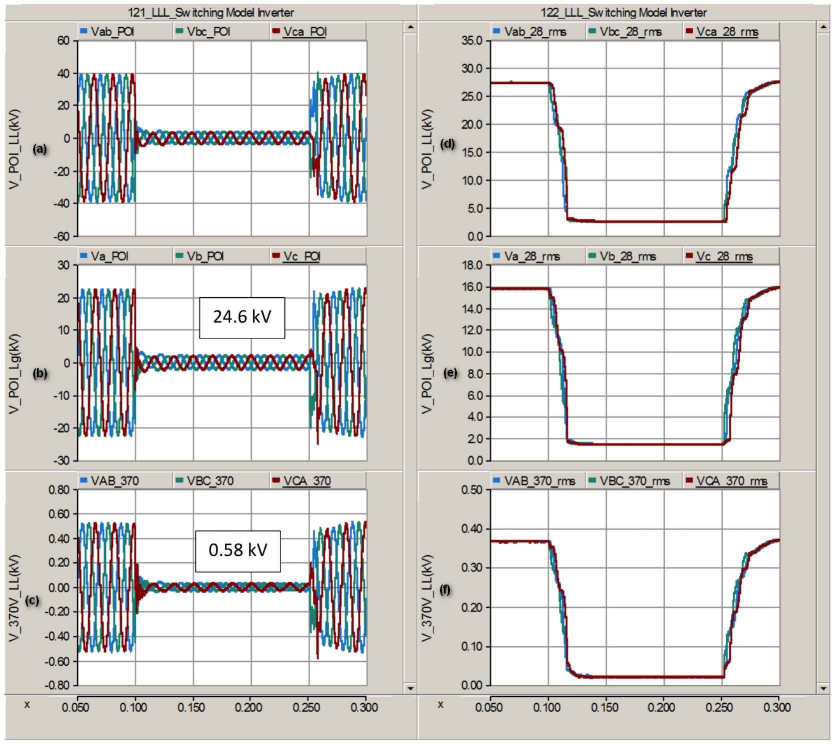

Figure 4.3: LLL Fault, Switched-model

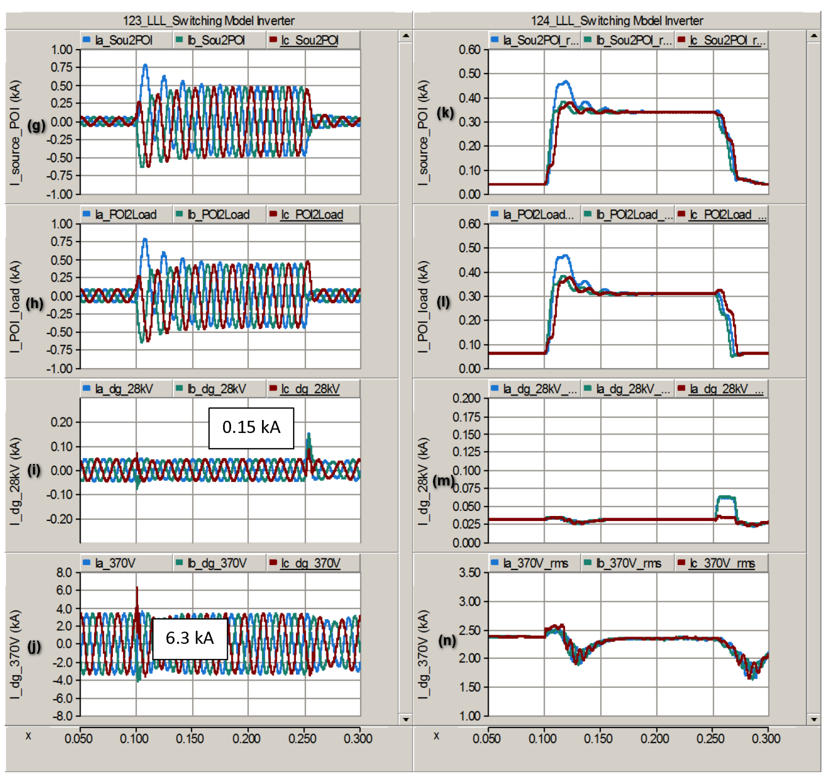

Figure 4.4: LLL Fault, Switched-model

Comparison of Figure 4.1 with the corresponding Figure 4.3 indicates that;

- Waveforms of line-to-line and line-to-ground voltages at POI are nearly the same. The peak values of the POI line-to-ground voltage, after the fault is cleared, are 26.3 kV for the current-injection model (Figure 4.1) and 24.6 kV for the switched-model (Figure4.3), respectively. Thus, the current-injection results in a higher peak value of POI line-to-ground voltage.

- During the system LLL fault, line-to-line voltages (at 370 V side) are different in Figure 4.1 and in Figure 4.3. Line-to-line voltages (at 370-V side) in Figure 4.1 have high frequency oscillations and the rms values of the three Line-to-line voltages are not equal either. When the fault occurs, the current-injection model, with respect to the rest of the system, is equivalent to a three-phase open-circuit and the high frequency oscillations are caused by the LC filter resonance. The switched-model during the fault is equivalent to a current-injecting voltage-source and thus do not exhibit the effect of system LC resonance. The recovery peak voltages after the LLL fault is cleared for the current-injection model and the switched-model are almost equal to 0.58-kV.

Comparison of Figure 4.2 with Figure 4.4 indicates that;

- The current waveforms (from source to POI) and (from POI to the load) are nearly the same. During the LLL fault, the major parts of these currents are flowing from the source to the fault, and the difference caused by the current-injection model and the switched-model are relatively insignificant.

- Amplitudes of the current waveforms (at VSC 27.6-kV side) in Figure 4.2 and 4.4 are nearly the same, but the waveforms in Figure 4.2 exhibit high frequency components. The reason is that during the LLL fault the current-injection model is equivalent to the three-phase open-circuit, so the LC filter causes the high frequency oscillations.

- The current peak values are 6.6 kA (in Figure 4.2) for the current-injection model and 6.3 kA (in Figure 4.4) for the switched-model. The waveforms in Figure 4.2 also exhibit higher frequency components.

Figure 4.1, 4.2, 4.3 and 4.4 conclude that both VSC models under the balanced RL load scenario, provide notably different transient responses due to LLL fault, and necessarily cannot be used interchangeably.

4.2.2 LG Fault

Figures 4.5 and 4.6 show the voltage and current waveforms respectively, for pre-fault, fault and post-fault periods when the VSC is represented by the current-injection model. Figures 4.7 and 4.8 show the voltage and current waveforms, for the same fault scenario, when the VSC is represented by the switched-model.

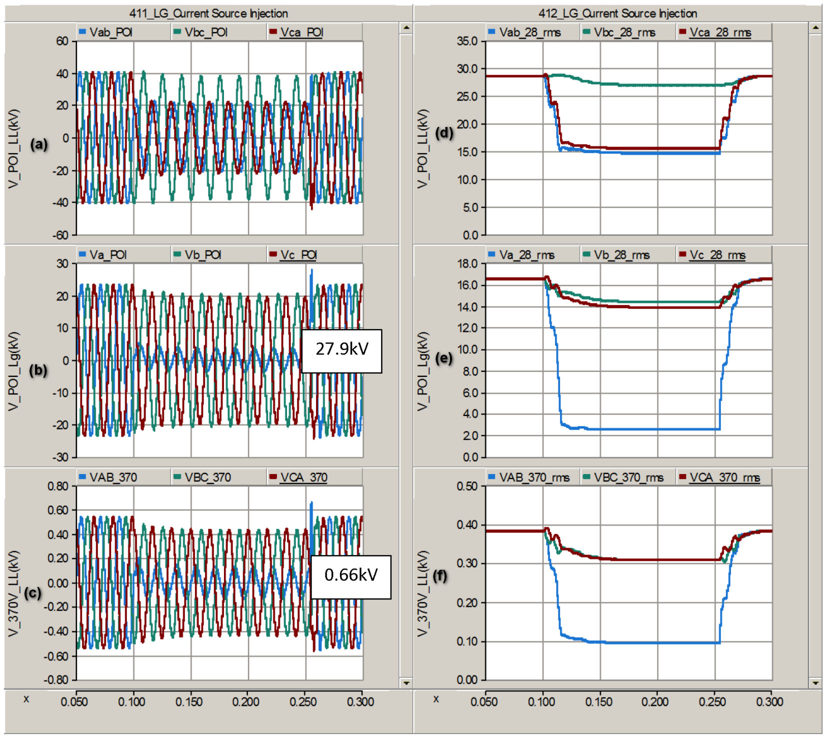

Figure 4.5: LG Fault, Current-Injection Model

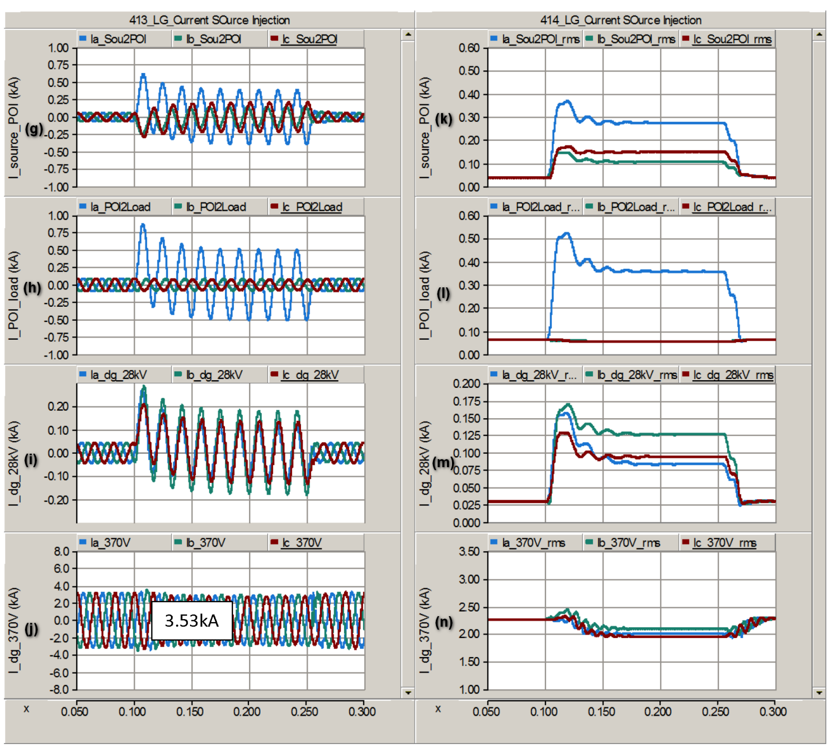

Figure 4.6: LG Fault, Current-Injection Model

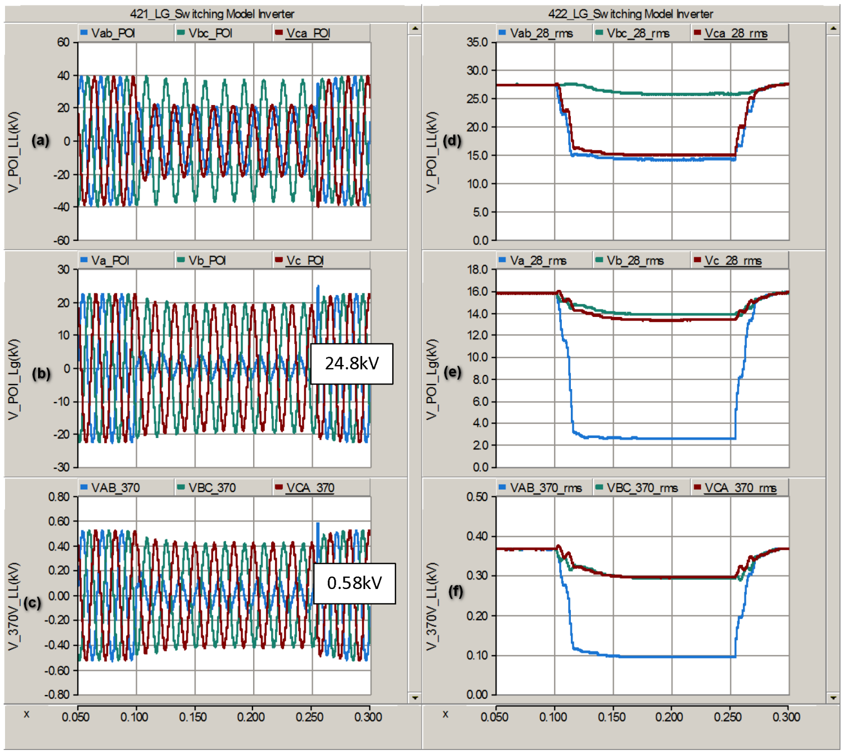

Figure 4.7: LG Fault, Switched-model

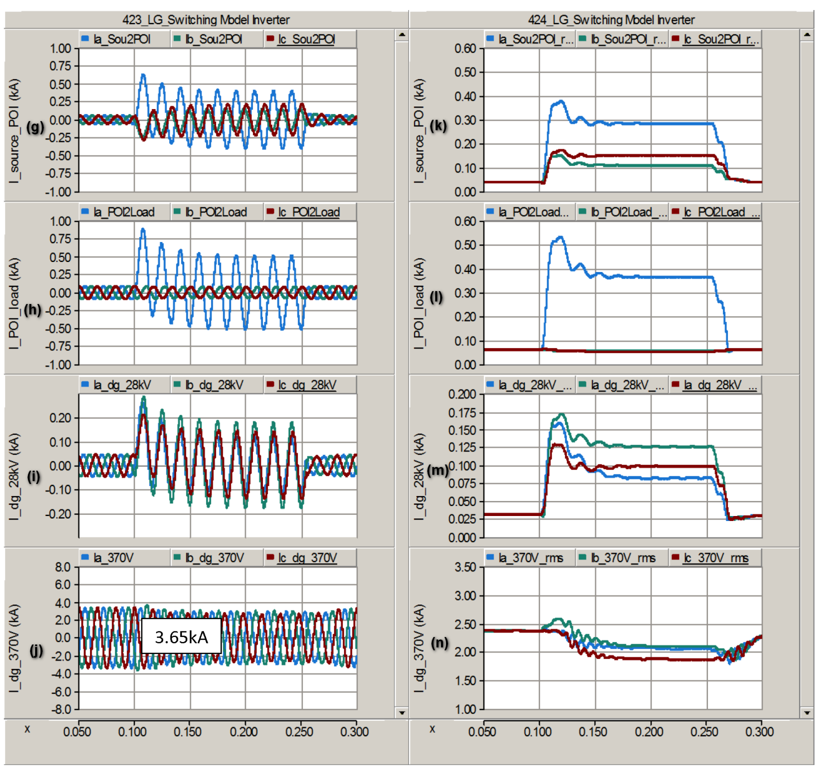

Figure 4.8: LG Fault, Switched-model

Comparison of Figures 4.5 and 4.7 conclude:

- The waveforms of line-to-ground voltages at POI nearly have the same patterns of variations for both models. The peak values of the recovery line-to-ground voltages at POI are 27.9 kV (Figure 4.5) for the current-injection model and 24.8 kV (Figure 4.7) for the switched-model, and the current-injection model results in significantly higher peak values of POI line-to-ground voltage.
- The peak values of the recovery voltages after the fault clearence are 0.66 kV (in Figure 4.5) and 0.58 kV (in Figure 4.7). Figure 4.5 also shows higher oscillations due to equivalent current source behaviour as explained in Section 4.2.1, page 56.

Comparison of the corresponding results in Figures 4.6 and 4.8 reveal that:

- The waveforms of currents (from the source to POI and the VSC 27.6-kV side) are almost the same for both models, and the difference in the peak values of the currents is negligiable.
- The peak values of current (at 370-V side) is 3.53 kA (Figure 4.6) for the current-injection model and 3.65 kA (Figure 4.8) for the switched-model.

Figures 4.5, 4.6, 4.7 and 4.8 conclude that both VSC models under the balanced RL load scenario, produce notably different results under the LG fault.

4.2.3 LLG Fault

Figures 4.9 and 4.10 show the voltage and current waveforms respectively, for the pre-fault, fault and post-fault periods when the VSC is represented by the current-injection model. Figures 4.11 and 4.12 show the voltage and current waveforms when the VSC is represented by the switched-model.

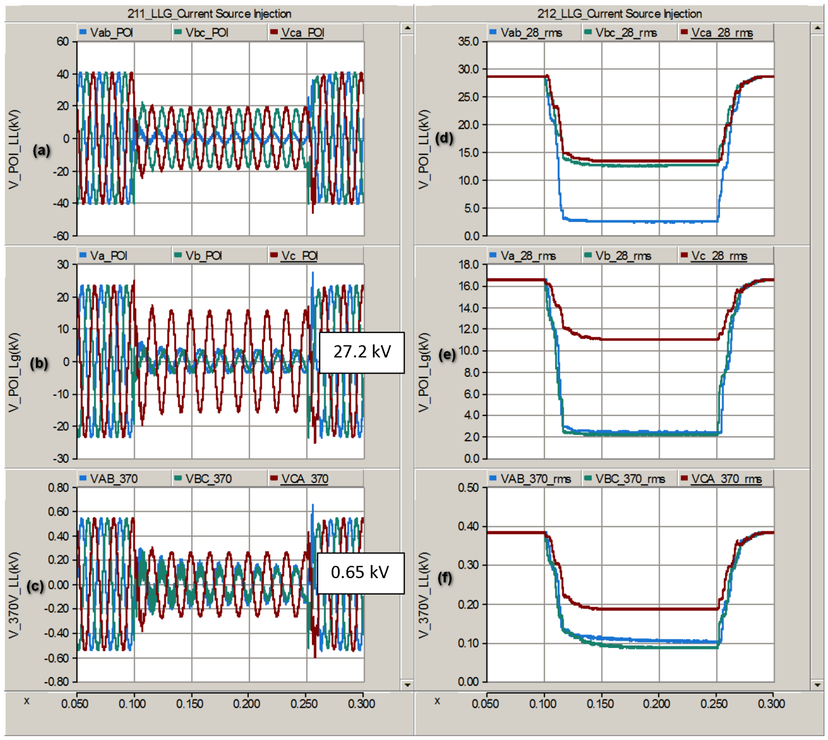

Figure 4.9: LLG Fault, Current-Injection model

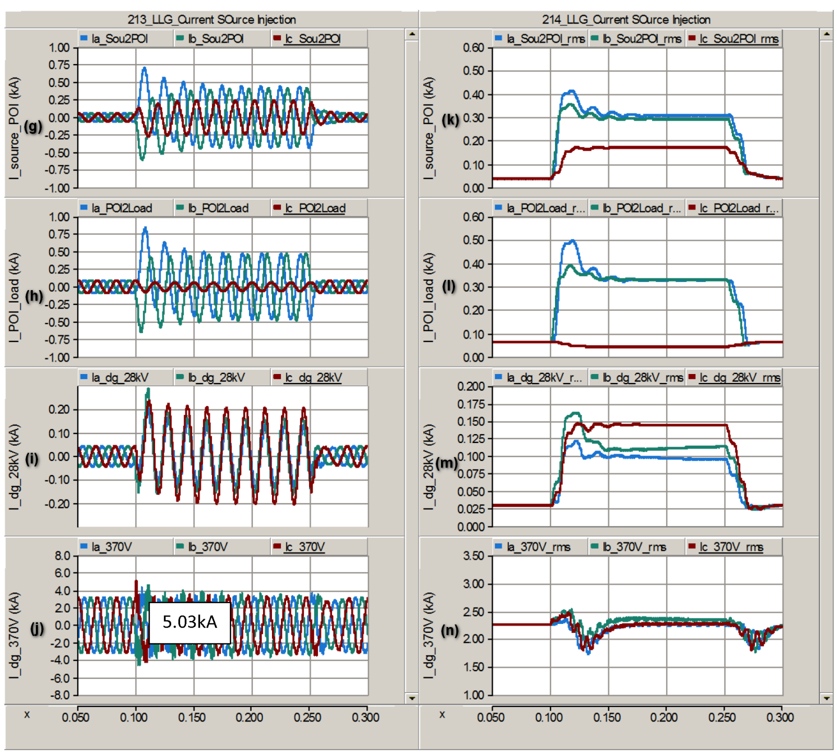

Figure 4.10: LLG Fault, Current-Injection model

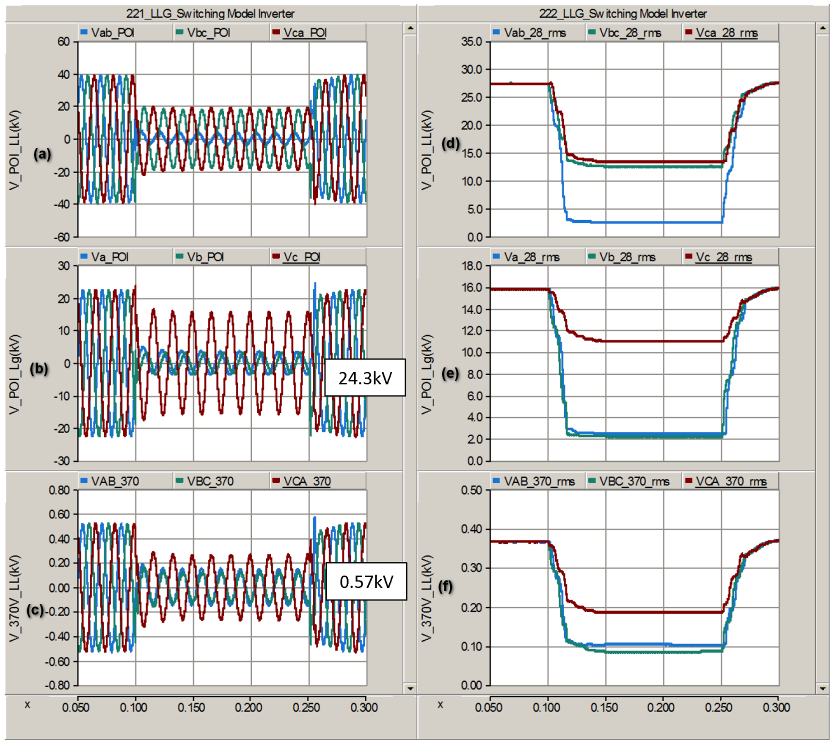

Figure 4.11: LLG Fault, Switched-model

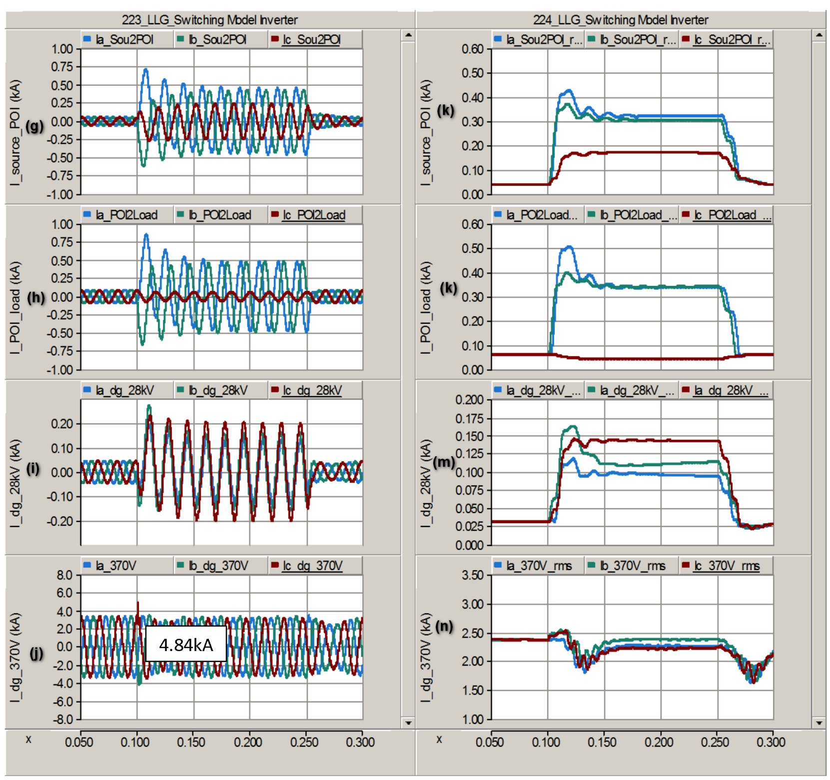

Figure 4.12: LLG Fault, Switched-model

Comparing to the corresponding waveforms from Figures 4.9 and 4.11 observes that:

- Instantaneous waveforms of the line-to-ground voltages at POI exhibit similar patterns of variation. However, the peak values of POI line-to-ground voltage is 27.2 kV (Figure 4.9) for the current-injection model and 24.3 kV (Figure 4.11) for the switched-model, and similar to the previous cases the current-injection model results in higher peak value.

- The line-to-line voltages (at 370-V side) are different. The line-to-line voltages (at 370-V side) of Figure 4.9 include higher oscillatory voltage components. Furthermore, the peak values of recovery voltages are 0.65 kV (Figure 4.9) and 0.57 kV (Figure 4.11), and the current-injection model results in higher peak values.

Comparison of the results from Figures 4.10 and 4.12 concludes:

- The current waveforms (from the source to POI and the VSC 27.6-kV side) are almost the same, and the differences in the peak values of the currents are negligiable.

- The peak values of currents (at 370-V side) are 5.03 kA (Figure 4.10) and 4.84 kA (Figure 4.12), and the waveforms in Figure 4.10 have high oscillatory components.

The study results of Figures 4.9 to 4.12 indicate the two VSC models, subject to the LLG fault, result in noticeably different results and cannot be used interchangeably.

4.2.4 LL Fault

Figures 4.13 and 4.14 show the voltage and current waveforms respectively, for the pre-fault, fault and post-fault periods when the VSC is represented by the current-injection model. Figures 4.15 and 4.16 show the voltage and current waveforms when the VSC is represented by the switched-model.

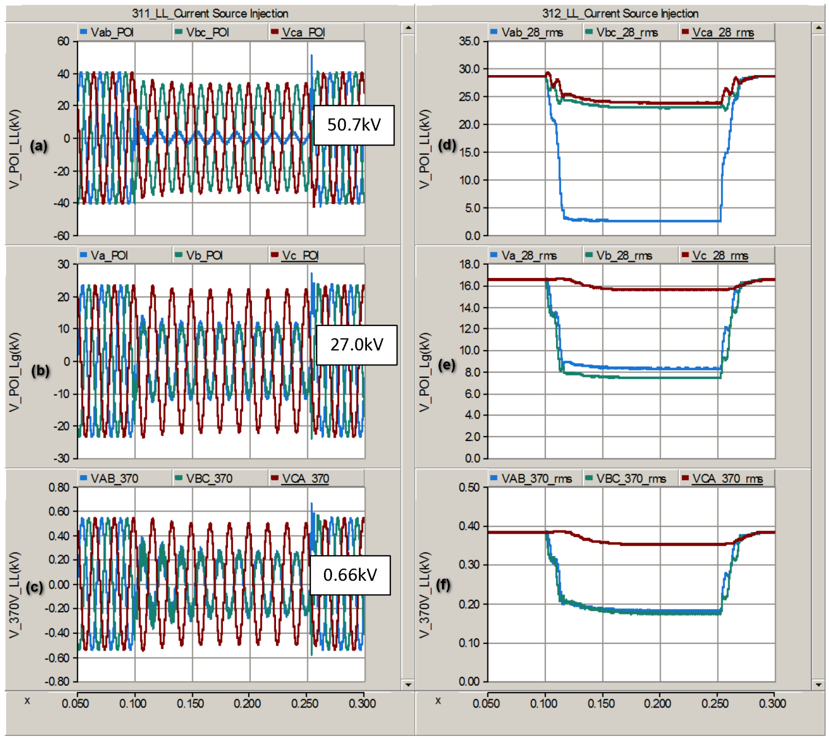

Figure 4.13: LL Fault, Current-Injection Model

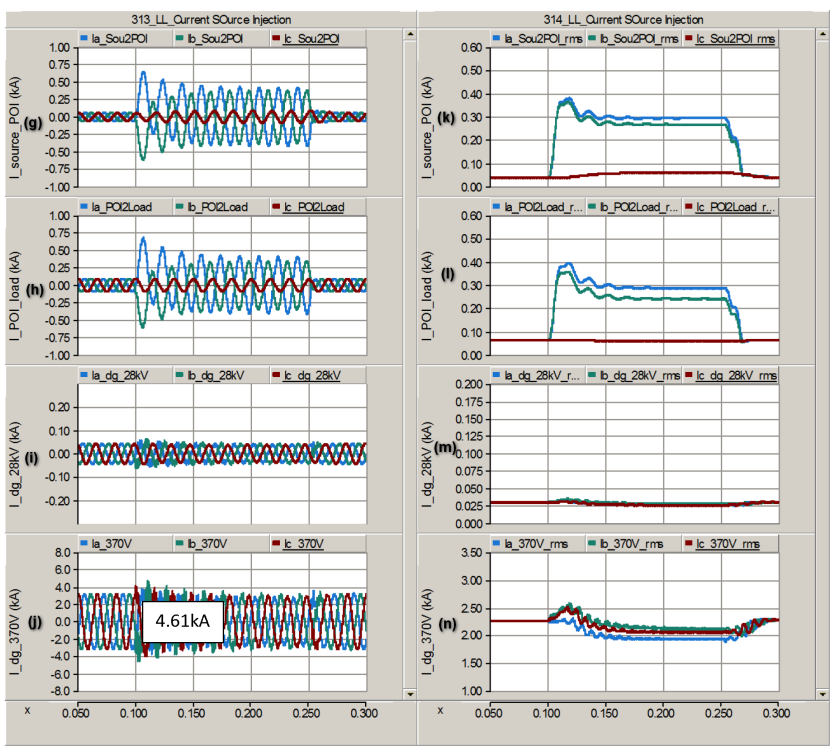

Figure 4.14: LL Fault, Current-Injection Model

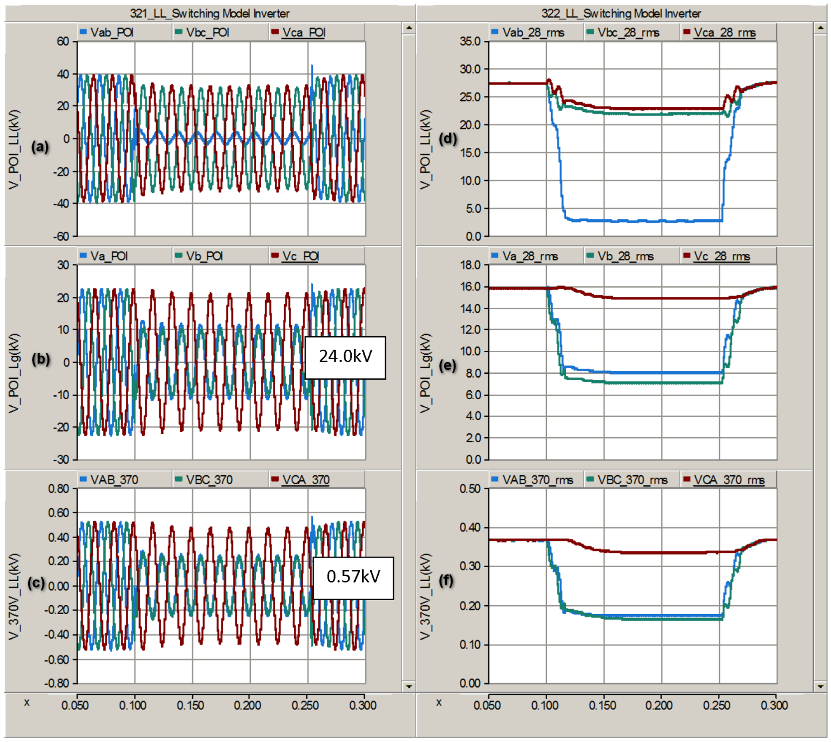

Figure 4.15: LL Fault, Switched-model

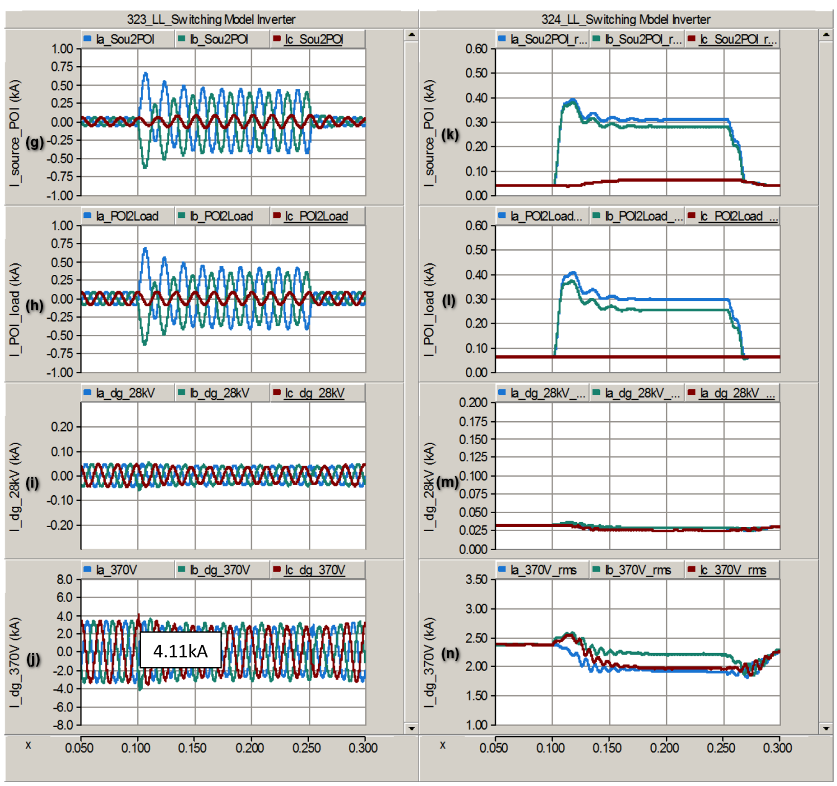

Figure 4.16: LL Fault, Switched-model

Comparison of the voltage waveforms (Figures 4.13 and 4.15) indicates that:

- Instantaneous waveforms of the line-to-ground voltages at POI exhibit similar patterns of variations, however, the peak value of the POI line-to-ground voltage is 27 kV (Figure 4.13) for the current-injection model and 24 kV (Figure 4.15) for the switched-model, and the current-injection model results in higher peak values.

- Comparing the line-to-line voltages (at 370-V side) in Figure 4.13 with those of Figure 4.15 shows that the line-to-line voltages in Figure 4.13 include higher oscillatory components. Another noticeable difference is that the peak value of the recovery voltage is 0.66 kV (Figure 4.13) for the current-injection and 0.57 kV (Figure 4.15) for the switched-model.

Comparison of Figure 4.14 and Figure 4.16 indicates that;

- The waveforms of currents (from the source to POI and the VSC 27.6-kV side) are almost the same, and the difference in the peak values are negligiable.

- The peak value of the current (at 370-V side) is 4.6 kA (Figure 4.6) for the current-injection model and 4.1 kA (Figure 4.8) for the switched-model.

Figures 4.13, 4.14, 4.15 and 4.16 conclude that both VSC models under the balanced RL load scenario, produce noticeably different results under the LL fault.

4.2.5 Effect of SCR on the Transient Responses of the VSC Models

The study results of Figures 4.1 to 4.16 correspond to the scenario when the short-circuit capacity of the POI is adjusted at 16.6 MVA. Similar studies to those Figures 4.1 to 4.16 also conducted when the SC_{MVA} was increased to 85 and reduced to 5. At higher values of SC_{MVA}, the waveforms of the corresponding currents and voltages produced by the two VSC models become more similar. However, the current-injection model always exhibits oscillatory components due to the resonance of the VSC filter.

As the short-circuit capacity of POI decreases, the corresponding waveforms of the two VSC models exhibit more pronounced differences. At $SC_{MVA} = 8$, the switched-model fails after the fault occurance. The reason for the failure is the significant harmonic content and distortion of the POI voltage which does not permit the PLL successfuly synchronize the VSC with the POI fundemental component. However, the current injection model can successfuly provide synchronization and operate after the fault inception. At $SC_{MVA} = 5$ both models fail and do not recover from the faulted condition. It should be noted that more ellaborate PLL structures can be used to operate the VSC for even lower SC_{MVA} values of the POI. These PLL structures are used for VSC-based HVDC converters, but as of now not adopted for distribution class VSC units.

4.3 Conclusions

This chapter evaluates and compares the corresponding time-domain responses of the switched-model and the current-injection model of the 1.5-MW VSC-interfaced DG unit under the feeder fault scenarios.Four fault scenarios, i.e., LLL, LG, LLG and LL are considered. Prior to a fault inception, the system is under balanced conditions and the imbalance is created due to the fault asymmetry. Each fault is a temporary fault for the duration of 0.15 s, and self-cleared at each phase current zero-crossing. The study results are obtained from time-domain simulation of the system in the PSCAD/EMTDC platform.

The reported simulation results of Fig. 4.1 to Fig. 4.16 show that:

- Although the patterns of variations of the corresponding waveforms from both models show similarity, however, the peak encountered values are noticeably different.
- The waveforms obtained from the current-injection model show oscillations due to resonance of the system inductance and the capacitor of the VSC AC-side filter. However, such oscillations are not observable in the switched-model responses. The reason is that the current-injection model behaves as a current source (open-circuit) during the fault transients and thus forces the filter capacitor to be in series with the system inductance. Thus oscillations at the natural frequency of the capacitor and the net system induce occur.
- The deviation between the corresponding waveforms of the two model become more significant as the SCR decreases, i.e., the system become "weaker".
- At SCR ≤ 8 the switched-model fails and cannot provide synchronization with the POI voltage. The reason is the significant distortion of the POI voltage due to harmonic and the voltage negative-sequence. The current-injection model can provide synchronization at SCR $= 8$ since it does not inject harmonics in the system. However, failure of the switched-model is a more realistic representation of the VSC unit and the results from the current-injection model are not reliable.
- For SCR values less than 5, both models fails due to the PLL failure to provide synchronization.

This chapter conclude that the results from the switched-model and the current-injection model, at SCR values of 16 or less, are noticeably different and the two models cannot be used interchangeably.

Chapter 5

Conclusions

This work provides a comprehensive performance evaluation an comparison of two models of the VSC-interfaced distributed resource units. The two models are the switched-model and the current-injection model. The switched-model represents detailed switching instants of the VSC electronic switches and thus provide accurate representation of the VSC and its control behaviour up to about 50 kHz. The current-injection model (also called current-sourced model) represent the VSC and its controlled by a three-phase current source that controls its injected current in the system based on the VSC inner-current control strategy. The current-injection model only injects the fundamental frequency current component in the system. The current-injection model is widely used by the electric power utilities and the VSC manufacturers/vendors to investigate the impact of VSC-interfaced distributed resource units on the utility grid. The main motivation of this work is to establish if the current-injection model accurately represents the steady-state and dynamic behaviours of the VSC unit under different SCR levels and degrees of system imbalance. The switched-model behaviour is used as the benchmark and basis to establish the degree of accuracy/validity of the current injection model.

The reported studies are conducted on a typical 27.6-kV distribution feeder which includes a 1.5-MW VSC-interfaced distributed generation unit. The studies are conducted based on time-domain simulation in the PSCAD/EMTDC platform.

The study results of the steady-state responses of the VSC models indicate that:

- When the SCR at the point of interconnection (POI) of the VSC unit is larger than 5, i.e., short-circuit capacity of the system is larger than 8.5-MVA, and the POI voltage imbalance within 2%, the current-injection model reproduces the same results (at the fundamental frequency) as those of the switched-model. Thus the two models can be used interchangeably.

- Under the above conditions, the presence of VSC unit can result in the high (67%) current unbalance, upstream to POI, which can violate the acceptable limits. However, this is a bi-product of the VSC-interfaced power generation property and not the model used to represent the VSC.

- When the SCR at POI becomes less than 5 and the voltage imbalance is within 2%, the difference between the corresponding results of the two VSC models become noticeable. The main reason is the impact of harmonics generated by the switched-model and the POI negative-sequence voltage on the behaviour of the VSC PLL. Since the current-injection does not generate harmonics, the corresponding PLL behaves "better". Thus, the results from the current-injection model are optimistic and necessarily not reliable.

- At very low SCR values, e.g., SCR ≤ 2, the switched-model fails to operate. This is due to inability of the PLL to provide proper synchronization. However, the current-injection model can provide synchronization. The inability of the VSC switched-model to operate is more realistic and the results from the VSC current-injection model are not acceptable.

The study results of extreme system conditions, fault conditions, show that:

- Although the patterns of variations of the corresponding waveforms from both models show similarity, however, the peak encountered values are noticeably different.
- The waveforms obtained from the current-injection model show oscillations due to resonance of the system inductance and the capacitor of the VSC AC-side filter. However, such oscillations are not observable in the switched-model responses. The reason is that the current-injection model behaves as a current source (open-circuit) during the fault transients and thus forces the filter capacitor to be in series with the system inductance. Thus oscillations at the natural frequency of the capacitor and the net system induce occur.
- The deviation between the corresponding waveforms of the two model become more significant as the SCR decreases, i.e., the system become "weaker".
- At SCR ≤ 8 the switched-model fails and cannot provide synchronization with the POI voltage. The reason is the significant distortion of the POI voltage due to harmonic and the voltage negative-sequence. The current-injection model can provide synchronization at SCR $= 8$ since it does not inject harmonics in the system. However, failure of the switched-model is a more realistic representation of the VSC unit and the results from the current-injection model are not reliable.
- For SCR values less than 5, both models fails due to the PLL failure to provide synchronization.

5.1 Contribution

The two main contributions of this work include:

- Clarifying that the current-injection model is a valid representation of the VSC steady-state, under unbalanced conditions, only for a specific range of SCR values.
- Establishing that the current-injection model is a valid representation of the VSC for a fairly limited range of SCR under fault scenarios.

5.2 Future Work

Potential future studies in continuation of this work can include:

- The range of validity of the current-injection model when multiple VSC units are represented by their corresponding current-injection models,
- potential modifications to the VSC unit control to mitigate the impact of system imbalance.

Appendix A

The Parameters of the Distribution Feeder

Table A.1: Appearent powers and Power Factors

Load names	S_A (kVA)	Pf_A	S_B (kVA)	Pf_B	S_C (kVA)	Pf_C
M1	2193.7	0.95	2193.7	0.95	2193.7	0.95
M2					160	0.95
M3			10	0.95		
M4	72	0.87	72	0.87	72	0.87
M5	274	0.87	274	0.87	274	0.87
M6	1099	0.95	946	0.95	1310	0.95
M7	256	0.75	256	0.75	256	0.75
M8	6.3	1	6.3	1	6.3	1
M9					20	0.95
M10	50	0.95	50	0.95	50	0.95
M11	170	0.95				
M12			25	0.95		
M13	217	1	217	1	217	1
M21					215	0.95
M25			85	0.95		

Table A.2: Active and Reactive Powers

Load names	P_A (kW)	Q_A (kVAr)	P_B (kW)	Q_B (kVAr)	P_C (kW)	Q_C (kVAr)
M1	2084	685	2084	685	2084	685
M2					160	0
M3			9.5	3.1		
M4	62.6	35.5	62.6	35.5	62.6	35.5
M5	238.38	135.1	238.38	135.1	238.38	135.1
M6	1044	343	899	295	1245	409
M7	192	169.3	192	169.3	192	169.3
M8	6.3		6.3		6.3	
M9					19	6.2
M10	47.5	15.6	47.5	15.6	47.5	15.6
M11	161	53.1				
M12			23.7	7.8		
M13	217		217		217	
M21					204.2	67.1
M25			80.7	26.5		

Table A.3: Resistive and Inductive Value of Loads

Load Bus Name	Load Name	VL_L	VL_G	R_a	R_b	R_c	X_a	X_b	X_c	L_a	L_b	L_c
		(kV)	(kV)	(Ohm)	(Ohm)	(Ohm)	(Ohm)	(Ohm)	(Ohm)	(H)	(H)	(H)
B1	M1 +M2 +M3	27.6	15.9	110.0	109.0	102.0	36.0	36.0	34.0	0.096	0.095	0.089
B2	M4+M5	27.6	15.9	638.0	638.0	638.0	362.0	362.0	362.0	0.960	0.960	0.960
B3	M6	8.3	4.8	20.0	23.0	17.0	7.0	8.0	5.0	0.017	0.020	0.015
B4	M7	27.6	15.9	744.0	744.0	744.0	656.0	656.0	656.0	1.740	1.740	1.740
B5	M8	27.6	15.9	40305.0	40305.0	40305.0						
B6	M9+ M10 +M11 +M12	27.6	15.9	1096.0	3216.0	3446.0	360.0	1057.0	1133.0	0.956	2.804	3.004
B7	M13	8.3	4.8	106.0	106.0	106.0						
B12	M21	27.6	15.9			1122.0			369.0			0.978
B15	M25	27.6	15.9		2838.0			933.0			2.474	

Table A.4: Line Parameters

Name of lines	Equipment ID	Length (m)
L1	336AL427	5700
L3	336AL427	400
L4	336AL427	380
L5	336AL427	130
L6	336AL427	170
L7	336AL427	260
L8	336AL427	140
L9	336AL427	380
L10	336AL427	560
L11	336AL427	300
L12	336AL427	3330
L13	336AL427	1030
L14	336AL427	1080
L15	336AL427	1640
L16	40ACRS427	470
L17	30ASR427	470
L18	4ACSR40	960
L19	40ACSR427	190
L20	30ASR427	1940
L22	30ASR427	1630
L26	30ASR427	2120
L30	40ACSR427	360
L31	40ACSR427	260
L32	10ASR2N	3580
L33	40ACSR427	770
L35	40ACSR427	4510
L36	336AL427	3240
L37	336AL427	300
L38	336AL427	500

Table A.5: NRCAN Overhead Line Parameters

Equipment ID	R1 (ohms/km)	X1 (ohms/km)	G1 (uS/km)	B1 (uS/km)	R0 (uS/km)	X0 (ohms/km)	G0 (uS/km)	B0 (uS/km)	Summer Rating (Amps)	Winter Rating (Amps)
10ASR2N	0.5356	0.5343	0	3.63	0.945	1.5081	0	1.91	301	301
336AL427	0.1696	0.3809	0	4.33	0.4689	1.2808	0	1.9	655	655
30ASR427	0.348	0.468	0	3.76	0.702	1.322	0	0	100	100
10ASR427	0.5523	0.4852	0	3.6	0.9644	1.461	0	1.92	321	321
40ACSR427	0.2697	0.4978	0	3.78	0.6055	1.3405	0	2.01	452	452
4ACSR40	1.3515	0.5359	0	3.36	1.7817	1.6524	0	1.82	172	172

Bibliography

[1] Ackermann, Thomas, Gran Andersson, and Lennart Sder. ”Distributed generation: a definition.” Electric power systems research 57, no. 3 (2001): 195-204.

[2] Purchala, K., R. Belmans, L. Exarchakos, and A. D. Hawkes. ”Distributed generation and the grid integration issues.” KULeuven, Imperial College London(2006).

[3] Bloemink, Jeffrey Michael. Validation of a Novel Approach to Voltage Sourced Converter Control for MicroGrid Applications. ProQuest, 2007.

[4] Midtsund, Tarjei. ”Control of Power Electronic Converters in Distributed Power Generation Systems: Evaluation of Current Control Structures for Voltage Source Converters operating under Weak Grid Conditions.” (2010).

[5] Kouro, Samir, Jose Leon, Dimitri Vinnikov, and Leopoldo G. Franquelo. ”Grid-Connected Photovoltaic Systems: An Overview of Recent Research and Emerging PV Converter Technology.” Industrial Electronics Magazine, IEEE 9, no. 1 (2015): 47-61.

[6] Hassaine, L., E. OLias, J. Quintero, and V. Salas. ”Overview of power inverter topologies and control structures for grid connected photovoltaic systems.”Renewable and Sustainable Energy Reviews 30 (2014): 796-807.

[7] Reed, Gregory, Ronald Pape, and Masatoshi Takeda. ”Advantages of voltage sourced converter (VSC) based design concepts for FACTS and HVDC-link applications.” In Power Engineering Society General Meeting, 2003, IEEE, vol. 3. IEEE, 2003.

[8] Yazdani, Amirnaser, and Reza Iravani. Voltage-sourced converters in power systems: modeling, control, and applications. John Wiley and Sons, 2010.

[9] Fortescue, Charles L. ”Method of symmetrical co-ordinates applied to the solution of polyphase networks.” American Institute of Electrical Engineers, Transactions of the 37, no. 2 (1918): 1027-1140.

[10] Gellings, Clark W. ”Power to the People.” Power and Energy Magazine, IEEE9, no. 5 (2011): 52-63.

[11] Chiniforoosh, S., J. Jatskevich, A. Yazdani, V. Sood, V. Dinavahi, J. A. Martinez, and A. Ramirez. ”Definitions and applications of dynamic average models for analysis of power systems.” Power Delivery, IEEE Transactions on 25, no. 4 (2010): 2655-2669.

[12] Mirhosseini, Mitra, Josep Pou, Baburaj Karanayil, and Vassilios Georgios Agelidis. "Positive-and negative-sequence control of grid-connected photovoltaic systems under unbalanced voltage conditions." In Power Engineering Conference (AUPEC), 2013 Australasian Universities, pp. 1-6. IEEE, 2013.

[13] Song, Hong-seok, and Kwanghee Nam. "Dual current control scheme for PWM converter under unbalanced input voltage conditions." Industrial Electronics, IEEE Transactions on 46, no. 5 (1999): 953-959.

[14] Zhao, Junhui, Caisheng Wang, Bo Zhao, Feng Lin, Quan Zhou, and Yang Wang. "A review of active management for distribution networks: current status and future development trends." Electric Power Components and Systems 42, no. 3-4 (2014): 280-293.

[15] Abdel-Galil, T. K., A. E. B. Abu-Elanien, E. F. El-Saadany, A. Girgis, Y. A. R. I. Mohamed, M. M. A. Salama, and H. H. M. Zeineldin. "Protection coordination planning with distributed generation." Qualsys Engco. Inc (2007).

[16] Chan, F.C. "Electrical Power Distribution Systems"(PDF). www.eolss.net.

[17] Graovac, Milan, Xiaolin Wang, Reza Iravani, and Chad Abbey. Integration of Storage in Electrical Distribution Systems and its Impact on the Depth of Penetration of DG. Technical Report CETC Number 2009-174/2009-10-21, Department of Electrical and Computer Engineering, University of Toronto, Prepared for: Chad Abbey, Natural Resources Canada, CANMET Energy Technology Centre, Quebec, May, 2008.

[18] Safigianni, Anastasia S., George N. Koutroumpezis, and Anastasios I. Spyridopoulos. "Distributed Generation Effects on Large-Scale Distribution Networks." Engineering 6, no. 01 (2014): 34.

[19] IEEE Std 1159 2009 IEEE Recommended Practice for Monitoring Electric Power Quality. 26 June 2009

[20] Lehn, Peter W. "Direct harmonic analysis of the voltage source converter." Power Delivery, IEEE Transactions on 18, no. 3 (2003): 1034-1042.

[21] Yazdani, Amirnaser. Modelling and Control of the Three-level Neutral Point Diode Clamped (NPC) Converter for High-power Applications. University of Toronto, 2005.

[22] Dugan, Roger C., Mark F. McGranaghan, and H. Wayne Beaty. "Electrical power systems quality." New York, NY: McGraw-Hill,— c1996 1 (1996).

[23] Chen, K., L. W. Montgomery, G. Klempner, J. Yagielski, J. Amos, M. Brimsek, and M. Sedlak. "Comparing IEEE 50.13 and IEC 60034 standards for large cylindrical rotor synchronous machines." In Power and Energy Society General Meeting, 2010 IEEE, pp. 1-9. IEEE, 2010.

[24] Stevenson, William D. Elements of power system analysis. Vol. 196, no. 2. New York: McGraw-Hill, 1982.

[25] Grainger, John J., and William D. Stevenson. Power system analysis. Vol. 31. New York: McGraw-Hill, 1994.

[26] Reddy, S. Chandrashekhar, G. Saritha, and N. Vikas. "Effect of distributed generation on distribution systems during faults." In Green Computing Communication and Electrical Engineering (ICGCCEE), 2014 International Conference on, pp. 1-9. IEEE, 2014.